

Evaporation of 2-Dimensional Black Holes

Abhay Ashtekar^{1,*} Frans Pretorius^{2,†} and Fethi M. Ramazanoğlu^{2‡}

¹ *Institute for Gravitation and the Cosmos & Physics Department, Penn State, University Park, PA 16802, USA*

² *Department of Physics, Princeton University, 08544, Princeton, NJ, USA*

We present a detailed analysis of results from a new study of the quantum evaporation of Callan-Giddings-Harvey-Strominger (CGHS) black holes within the mean-field approximation. This semi-classical theory incorporates back reaction. Our analytical and numerical calculations show that, while some of the assumptions underlying the standard evaporation paradigm are borne out, several are not. One of the anticipated properties we confirm is that the semi-classical space-time is asymptotically flat at right future null infinity, \mathcal{I}_R^+ , yet incomplete in the sense that null observers reach a future Cauchy horizon in finite affine time. Unexpected behavior includes that the Bondi mass traditionally used in the literature can become negative even when the area of the horizon is macroscopic; an improved Bondi mass remains positive until the end of semi-classical evaporation, yet the final value can be arbitrarily large relative to the Planck mass; and the flux of the quantum radiation at \mathcal{I}_R^+ is non-thermal even when the horizon area is large compared to the Planck scale. Furthermore, if the black hole is initially macroscopic, the evaporation process exhibits remarkable universal properties. Although the literature on CGHS black holes is quite rich, these features had escaped previous analyses, in part because of lack of required numerical precision, and in part due to misinterpretation of certain properties and symmetries of the model. Finally, our results provide support for the full quantum scenario recently developed by Ashtekar, Taveras and Varadarajan, and also offer a number of interesting problems to the mathematical relativity and geometric analysis communities.

PACS numbers: 04.70.Dy, 04.60.-m, 04.62.+v, 04.60.Pp

I. INTRODUCTION

Although literature on the quantum nature of black holes is vast, many important questions on the dynamics of their evaporation still remain unanswered. This is true even for 2-dimensional models, introduced some twenty years ago [1–3]. In this paper, as a follow up to [4], we present a detailed analysis of the semi-classical dynamics of 2-dimensional, Callan-Giddings-Harvey-Strominger (CGHS) black holes [1], using a combination of analytical and high precision numerical methods. This model has been studied extensively in the past [2]. Yet we find new and rather remarkable behavior for classes of black holes where the collapse is prompt and the Arnowitt-Deser-Misner (ADM) mass is large: As these black holes evaporate, after an initial transient phase, dynamics of various physically interesting quantities flow to universal curves. In addition, this analysis brings out certain unforeseen limitations of the standard paradigm that has been used to discuss black hole evaporation for some two decades. The overall situation bares interesting parallels to the discovery of critical phenomena at the threshold of gravitational collapse in classical general relativity [5, 6]; at the time it was assumed that the spherically symmetric gravitational collapse problem was essentially “solved”, yet all earlier work had missed this very rich and profound property of gravitational collapse. Also, it served as a new example of rather simple, universal behavior that dynamically emerges from a complicated system of non-linear partial differential equations. Here, though the physical scenario is different, a similar unexpected universal behavior

arises. This universality strongly suggests that, although the S-matrix is very likely to be unitary, all the information in the infalling matter will not be imprinted in the outgoing quantum state. As discussed in detail in the paper, this mismatch between unitarity and information recovery is a peculiarity of 2 dimensions.

Our investigation is carried out within the mean-field approximation of [7] in which the black hole formation and evaporation is described entirely in terms of non-linear, partial differential equations (PDEs). Thus there will be no Hilbert spaces, operators or path integrals in this paper.¹ The focus is rather on the consequences of the geometrical PDEs governing black hole evaporation in the semi-classical regime, and the intended audience is mathematical and numerical relativists. Therefore we will start with an introductory review of the CGHS model—the classical field theory in Sec. IA and semi-classical corrections in Sec. IB—and then summarize the results and outline the rest of the paper in Sec. IC.

A. The Classical CGHS Model

Consider first the spherical collapse of a massless scalar field f in 4 space-time dimensions. Mathematically, it is convenient to write the coordinate r which measures the physical radius of metric 2-spheres as $r = e^{-\phi}/\kappa$ where κ is a constant with dimensions of inverse length. The space-time

* ashtekar@gravity.psu.edu

† fpretori@princeton.edu

‡ framazan@princeton.edu

¹ This paper complements a companion article [8] which is primarily devoted to quantum issues, particularly that of potential information loss, and another companion article [9] devoted to the details of numerical simulations.

metric ${}^4g_{ab}$ can then be expressed as

$${}^4g_{ab} = \underline{g}_{ab} + r^2 s_{ab} := \underline{g}_{ab} + \frac{e^{-2\phi}}{\kappa^2} s_{ab}, \quad (1.1)$$

where s_{ab} is the unit 2-sphere metric and \underline{g}_{ab} is the 2-metric in the r - t plane. In terms of these fields, the action for this Einstein-Klein-Gordon sector can be written as

$$\tilde{S}(\underline{g}, \phi, f) = \frac{1}{8\pi G_4} \frac{4\pi}{\kappa^2} \int d^2x \sqrt{|\underline{g}|} e^{-2\phi} (\underline{R} + 2\nabla^a \phi \nabla_a \phi + 2e^{-2\phi} \kappa^2) - \frac{1}{2} \int d^2x \sqrt{|\underline{g}|} e^{-\phi} \nabla^a f \nabla_a f \quad (1.2)$$

where G_4 is the 4-dimensional Newton's constant, ∇ is the derivative operator and \underline{R} the scalar curvature of the 2-metric \underline{g}_{ab} . The CGHS model, by contrast refers to gravitational collapse of a scalar field in 2 space-time dimensions. The gravitational field is now coded in a 2-metric \underline{g}_{ab} and a dilaton field ϕ , and the theory has a 2-dimensional gravitational constant G of dimensions $[ML]^{-1}$ in addition to the constant κ of dimensions $[L]^{-1}$ (κ^2 is sometimes regarded as the cosmological constant).² The CGHS action is given by [1]:

$$S(\underline{g}, \phi, f) = \frac{1}{G} \int d^2x \sqrt{|\underline{g}|} e^{-2\phi} (\underline{R} + 4\nabla^a \phi \nabla_a \phi + 4\kappa^2) - \frac{1}{2} \int d^2x \sqrt{|\underline{g}|} \nabla^a f \nabla_a f. \quad (1.3)$$

Note that the two actions are closely related. The only difference is in some coefficients which appear bold faced in (1.2). This is why one expects that analysis of the CGHS model should provide useful intuition for evaporation of spherically symmetric black holes in 4 dimensions.

On the other hand, the two theories do differ in some important ways and we anticipate that only certain aspects of universality will carry over to 4-dimensions. These differences are discussed in section IV. Here, we only note one: since the dilaton field does not appear in the scalar field action of (1.3), dynamics of f decouples from that of the dilaton. Now, since our space-time is topologically \mathbb{R}^2 , the physical 2-metric \underline{g}_{ab} is conformally flat. We can thus fix a fiducial flat 2-metric η^{ab} and write $\underline{g}^{ab} = \underline{\Omega} \eta^{ab}$, thereby encoding the physical geometry in the conformal factor $\underline{\Omega}$ and the dilaton field ϕ . Next, since the wave equation is conformally invariant,

$$\square(\underline{g})f = 0 \quad \Leftrightarrow \quad \square(\eta)f = 0, \quad (1.4)$$

f is only subject to the wave equation in the fiducial flat space which can be easily solved, without any knowledge of the physical geometry governed by $(\underline{\Omega}, \phi)$. *This is a key simplification which is not shared by the scalar field f in the spherically symmetric gravitational collapse described by (1.2).* Denote by z^\pm the advanced and retarded null coordinates of η so that $\eta_{ab} = 2\partial_{(a} z^+ \partial_{b)} z^-$. Then a general solution to (1.4) on the fiducial Minkowski space (M^o, η) is simply

$$f(z^\pm) = f_+(z^+) + f_-(z^-) \quad (1.5)$$

² In this paper we set $c = 1$ but keep Newton's constant G and Planck's constant \hbar free. Note that since $G\hbar$ is a *Planck number* in 2 dimensions, setting both of them to 1 is a physical restriction.

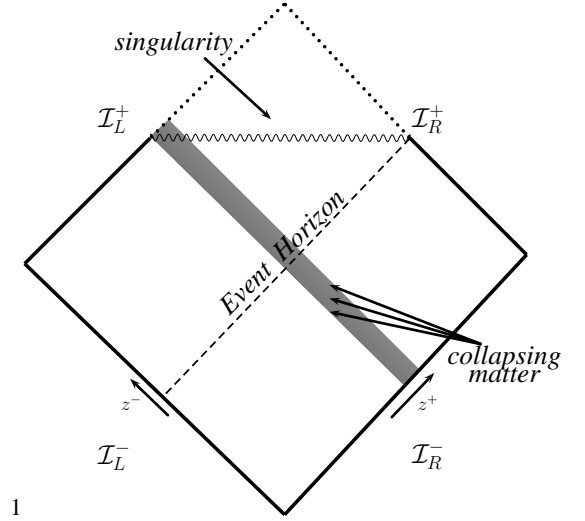


Figure 1. Penrose diagram of the CGHS black hole formed by the gravitational collapse of a left moving field f_+ . The physical space-time is that part of the fiducial Minkowski space which is to the past of the space-like singularity.

where f_\pm are arbitrary well behaved functions of their arguments. In the classical CGHS theory, one sets $f_- = 0$ and focuses on the gravitational collapse of the left moving mode f_+ . As one might expect, the true degree of freedom lies only in f_+ , i.e., f_+ completely determines the geometry. But in the classical CGHS model, there is a further unexpected simplification: *the full solution can be expressed as an explicit integral involving f_+ !*

For later purposes, following [7], let us set

$$\underline{\Phi} := e^{-2\phi}$$

and introduce a new field $\underline{\Theta}$ via

$$\underline{\Theta} = \underline{\Omega}^{-1} \underline{\Phi} \quad \text{so that} \quad g^{ab} = \underline{\Theta}^{-1} \underline{\Phi} \eta^{ab}$$

Then the geometry is completely determined by the pair of fields $\underline{\Theta}, \underline{\Phi}$, and field equations obtained by varying (1.3) can be solved to express $\underline{\Theta}, \underline{\Phi}$ directly in terms of f_+ . The resulting expressions for $\underline{\Theta}$ and $\underline{\Phi}$ are simpler in terms of 'Kruskal-like' coordinates x^\pm given by

$$\kappa x^+ = e^{\kappa z^+}, \quad \text{and} \quad \kappa x^- = -e^{-\kappa z^-}. \quad (1.6)$$

Given any regular f_+ , the full solution to the classical CGHS equations can now be written as

$$\begin{aligned} \underline{\Theta} &= -\kappa^2 x^+ x^- \\ \underline{\Phi} &= \underline{\Theta} - \frac{G}{2} \int_0^{x^+} d\bar{x}^+ \int_0^{\bar{x}^+} d\bar{x}^- (\partial f_+ / \partial \bar{x}^+)^2. \end{aligned} \quad (1.7)$$

Note that, given any regular f , the fields $(\underline{\Theta}, \underline{\Phi})$ of (1.7) that determine geometry are also regular everywhere on the fiducial Minkowski manifold M^o .

How can the solution then represent a black hole? It turns out that, for any regular f_+ , the field $\underline{\Phi}$ of (1.7) vanishes along

a space-like line ℓ_s . Along ℓ_s then, \mathbf{g}^{ab} vanishes, whence the covariant metric \mathbf{g}_{ab} fails to be well-defined. It is easy to verify that the Ricci scalar of \mathbf{g}_{ab} diverges there. This is the singularity of the physical metric \mathbf{g} . The physical space-time (M, \mathbf{g}_{ab}) occupies only that portion of M^o which is to the past of this singularity (see Fig. 1).

But does ℓ_s represent a black hole singularity? It is easy to check that (M, \mathbf{g}_{ab}) admits a smooth null infinity \mathcal{I} which has 4 components (because we are in 2 space-time dimensions): \mathcal{I}_L^- and \mathcal{I}_R^- coincide with the corresponding \mathcal{I}_L^{o-} and \mathcal{I}_R^{o-} of Minkowski space-time (M^o, η) while \mathcal{I}_L^+ and \mathcal{I}_R^+ are proper subsets of the Minkowskian \mathcal{I}_L^{o+} and \mathcal{I}_R^{o+} . Nonetheless, \mathcal{I}_R^+ is complete with respect to the physical metric \mathbf{g}_{ab} and its past does not cover all of M . Thus, there is indeed an event horizon with respect to \mathcal{I}_R^+ hiding a black hole singularity. However, unfortunately \mathcal{I}_L^+ is not complete with respect to \mathbf{g}_{ab} . Therefore, strictly speaking we cannot even ask³ if there is an event horizon—and hence a black hole—with respect to \mathcal{I}_L^+ ! Fortunately, it turns out that for the analysis of black hole evaporation—and indeed for the issue of information loss in full quantum theory—only \mathcal{I}_R^+ is relevant. To summarize then, even though our fundamental mathematical fields (Θ, Φ) are everywhere regular on full M^o , a black hole emerges because physics is determined by the Lorentzian geometry of \mathbf{g} .

Although a black hole does result from gravitational collapse in the CGHS model, it follows from the explicit solution (1.7) that one does not encounter all the rich behavior associated with spherical collapse in 4 dimensions. In particular there are no critical phenomena [5, 6], essentially because there is no threshold of black hole formation: a black hole results no matter how weak the infalling pulse f_+ is. However, as remarked in the beginning of this section, the situation becomes more interesting even in this simple model once one allows for quantum evaporation and takes into account its back reaction.

B. The Semi-Classical CGHS Model

To incorporate back reaction, one can use semi-classical gravity where matter fields are allowed to be quantum but geometry is kept classical. In this paper we will implement this idea using the mean field approximation of [7, 8] where one ignores the quantum fluctuations of geometry—i.e., of quantum fields $(\hat{\Theta}, \hat{\Phi})$ —but keeps track of the quantum fluctuations of matter fields. The validity of this approximation requires a large number of matter fields \hat{f}_i , with $i = 1, \dots, N$ (whence it is essentially the large N approximation [1, 2]). Then, there is a large domain in space-time where quantum fluctuations of matter can dominate over those of geometry. Back reaction of the quantum radiation modifies classical equations with terms proportional to $NG\hbar$. However, dynamics of the physical metric g is again governed by PDEs

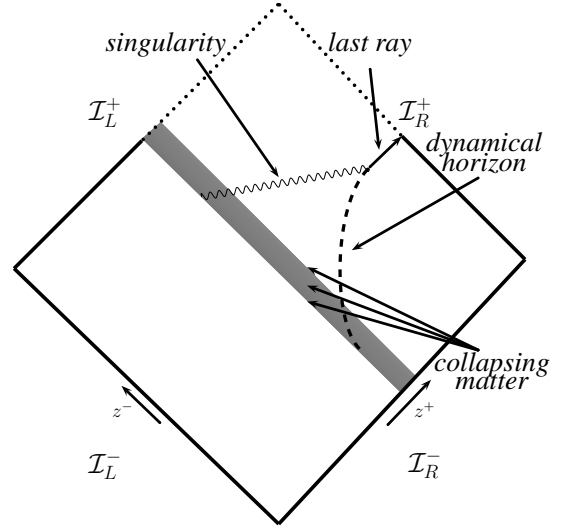


Figure 2. Penrose diagram of an evaporating CGHS black hole in the mean field approximation. Because of quantum radiation the singularity now ends in the space-time interior and does not reach \mathcal{I}_L^+ or \mathcal{I}_R^+ (compare with Fig. 1.) Space-time admits a generalized dynamical horizon whose area steadily decreases. It meets the singularity at its (right) end point. The physical space-time in this approximation excludes a future portion of the fiducial Minkowski space (bounded by the singularity, the last ray and the future part of the collapsing matter).

on classical fields, (Θ, Φ) , which we write without an underbar to differentiate them from solutions $(\underline{\Theta}, \underline{\Phi})$ to the classical equations ($N\hbar = 0$). In the domain of applicability of the mean-field approximation, they are given by expectation values of the quantum operator fields: $\Theta = \langle \hat{\Theta} \rangle$ and $\Phi = \langle \hat{\Phi} \rangle$. The difference from the classical case is that the coefficients of the PDEs and components of the metric g_{ab} now contain \hbar .

For any given finite N , there is nonetheless a region in which the quantum fluctuations of geometry are simply too large for the mean field approximation to hold. This is reflected in the fact that a singularity persists in this approximation, although it is now weakened. The field Φ now assumes a non-zero value $NG\hbar/12$ at the singularity whence g^{ab} is invertible there [2]. Furthermore it is C^0 across this singularity but not C^1 . Finally, because of back-reaction, the strength of the singularity diminishes as the black hole evaporates and the singularity ends in the interior of space-time; in contrast to the classical singularity, it does not reach \mathcal{I}_R^+ (see Fig. 2). It is the dynamics of g_{ab} that exhibit novel, universal features.

It turns out that the fundamental equations of the mean-field theory (and in fact also of the full quantum theory [7, 8]) admit a *scaling symmetry*, which was discovered independently by Ori [11]. This has important consequences, which to our knowledge have not been fully appreciated before.⁴ It naturally leads to certain physical quantities that have universal

³ Even in 4-dimensions, the black hole region is defined as $\mathcal{B} := M \setminus J^-(\mathcal{I}^+)$ provided \mathcal{I}^+ is complete. If we drop the completeness requirement, even Minkowski space would admit a black hole! See, e.g., [10].

⁴ In [12] for example it was noted that N could be “scaled out” of the problem and that the results are “qualitatively independent of N ”. However, as

properties during and at the end of the quantum evaporation of large black holes. Unraveling this unforeseen behavior requires the use of an appropriate analytical formulation of the problem, and high precision numerical solutions (both in terms of requiring small truncation error and using the full range of 16-digit double precision floating point arithmetic)—for details, see the companion papers [8, 9]. These universal properties have their origin in the PDEs governing the dynamics. Therefore, our numerical results lead to a series of interesting conjectures in mathematical relativity and geometric analysis (discussed in section IV). In addition our detailed analysis shows, quite surprisingly, that several of the standard assumptions that have driven the quantum evaporation paradigm are incorrect. As a consequence, results of this paper also play a significant role in resolving the information loss puzzle in the quantum theory [7, 8].

C. Summary of New Results

To summarize the new results, let us first recall the standard paradigm. Literature on the quantum evaporation of CGHS black holes uses a certain definition of Bondi mass $M_{\text{Bondi}}^{\text{Trad}}$. Essentially every preceding paper assumed that: i) The semi-classical approximation is excellent until the horizon shrinks to Planck size; ii) Throughout this long phase, $M_{\text{Bondi}}^{\text{Trad}}$ is non-negative and the process is quasi-static; iii) Consequently, during this phase the quantum flux at \mathcal{I}_R^+ is given by the Hawking thermal flux and the semi-classical approximation holds; and iv) At the end of this phase the Bondi mass is also of Planck size. It is then difficult to imagine how purity of the incoming quantum state could be preserved in the outgoing state. However, our results show that several features of this scenario fail to be borne out by detailed calculations in the semi-classical theory. In particular, in section III we will show the following results for a prompt collapse of data with large ADM mass:

- The traditional Bondi mass, $M_{\text{Bondi}}^{\text{Trad}}$, in fact becomes *negative* (and large) even while the horizon area is macroscopic.
- The definition of $M_{\text{Bondi}}^{\text{Trad}}$ is taken directly from the classical theory where the black hole is static. Now, in 4-dimensions one knows [13] that the formula for the Bondi mass has to be modified in non-stationary space-times (from $\oint \Psi_2^2 d^2V$ to $\oint (\Psi_2^2 - \sigma\bar{\sigma}) d^2V$). Indeed if one were to ignore this modification, one would find that neither the Bondi mass nor the Bondi flux is always positive. By mimicking the 4-d procedure, Ashtekar, Taveras and Varadarajan (ATV) [7] had proposed a quantum corrected Bondi mass, $M_{\text{Bondi}}^{\text{ATV}}$, in

the CGHS mean-field theory (which, in particular, reduces to $M_{\text{Bondi}}^{\text{Trad}}$ in the classical theory). This mass remains *positive* throughout the evaporation process of the mean-field approximation.

- Although the horizon area goes to zero at the end of the evaporation process in the mean-field approximation, $M_{\text{Bondi}}^{\text{ATV}}$ is *not* of Planck size at that time (i.e., at the point where the ‘last ray’ of Fig.2 intersects \mathcal{I}_R^+). For all black holes with large initial ADM mass, as the horizon area shrinks to zero $M_{\text{Bondi}}^{\text{ATV}}$ approaches a *universal* value $\approx 0.864\bar{N}$ in Planck units, with $\bar{N} = N/24$. This end point Bondi mass is macroscopic since N is necessarily large in the semi-classical theory.
- Dynamics *during* the evolution process also shows a *universal behavior*. For example, one can calculate $M_{\text{Bondi}}^{\text{ATV}}$ as a function of the horizon area a_{hor} . There is a transient phase immediately after the horizon is first formed, though after that the plot of $M_{\text{Bondi}}^{\text{ATV}}$ against a_{hor} joins a universal curve all the way to zero area.
- The flux of energy radiated across \mathcal{I}_R^+ departs from the thermal flux when $M_{\text{Bondi}}^{\text{ATV}}$ and even a_{hor} are macroscopic.
- Although the Ricci scalar of the mean-field metric g diverges at the (weak) singularity, it is regular on the last ray and goes to zero as one approaches \mathcal{I}_R^+ along this ray. Thus, contrary to a wide spread belief, there is no ‘thunderbolt’ curvature singularity in the semi-classical theory.

We will see in section IV C that our results strongly suggest that the S matrix from \mathcal{I}_L^- to \mathcal{I}_R^+ is likely to be unitary. However, *because of the universality* of physical quantities at \mathcal{I}_R^+ , it is very unlikely that information in the infalling matter at \mathcal{I}_R^- will be recovered in the outgoing state at \mathcal{I}_R^+ . This is in sharp contrast with a wide-spread expectation; indeed, mechanisms for information recovery have been suggested in the past (see e.g. [14]). This expectation illustrates the degree to which universality was unanticipated in much of the CGHS literature.

The rest of this paper is organized as follows. In section II we summarize the mean-field theory of [7, 8], introduce the scaling behavior and explain the subtleties associated with Planck units in 2 dimensions. This framework provides the basis for the numerical results discussed in III. These results are more extensive than the brief summary presented above. Finally in section IV we discuss the ramifications of these results and list interesting problems they suggest in geometric analysis.

II. THE MEAN-FIELD APPROXIMATION

This section is divided into three parts. We recall (mainly from [2, 7, 8]) the PDEs that govern semi-classical gravity in the first part and their consequences in the second. In the third

we will discuss in Sec. II B, it is actually the ratio M_{ADM}/N which classifies a solution, and more importantly there is qualitatively different behavior in the small (Planck size) vs. large (macroscopic) M_{ADM}/N limits. In this terminology, the simulation of [12] corresponds to an initially Planck size black hole.

we introduce a scaling symmetry which leads to a natural distinction between macroscopic and Planck scale black holes.

A. mean-field equations

As mentioned in section I, in semi-classical gravity we have N quantum scalar fields $\hat{f}^{(i)}$, with $i = 1 \dots N$. In the mean-field approximation, we capture the idea that it is only the left moving modes that undergo gravitational collapse by choosing the initial state appropriately: we let this state be the vacuum state for the right moving modes $\hat{f}_-^{(i)}$ and a coherent state peaked at any given classical profile f_+^o for each of the N left moving fields $\hat{f}_+^{(i)}$. This specification at \mathcal{I}^- defines a (Heisenberg) state $|\Psi\rangle$. Dynamical equations are obtained by taking expectation values of the quantum evolution equations for (Heisenberg) fields in this state $|\Psi\rangle$ and ignoring quantum fluctuations of geometry but not of matter. Technically, this is accomplished by substituting polynomials $P(\hat{\Theta}, \hat{\Phi})$ in the geometrical operators with polynomials $P(\langle\hat{\Theta}\rangle, \langle\hat{\Phi}\rangle) := P(\Phi, \Theta)$ of their expectation values. For the matter fields $\hat{f}^{(i)}$, on the other hand, one does not make this substitution; one keeps track of the quantum fluctuations of matter. These lead to a conformal anomaly: While the trace of the stress-tensor of scalar fields vanishes in the classical theory due to conformal invariance, the expectation value of this trace now fails to vanish. Therefore equations of motion of the geometry acquire new source terms of quantum origin which modify its evolution.

To summarize, then, in the mean-field approximation the dynamical objects are again just smooth fields f_i, Θ, Φ (representing expectation values of the corresponding quantum fields). While there are N matter fields, geometry is still encoded in the two basic fields Θ, Φ which determine the space-time metric g^{ab} via $g^{ab} = \Omega \eta^{ab} := \Theta^{-1} \Phi \eta^{ab}$. Dynamics of $f^{(i)}, \Theta, \Phi$ are again governed by PDEs but, because of the trace anomaly, equations governing Θ, Φ acquire quantum corrections which encode the back reaction of quantum radiation on geometry.

As in 4-dimensional general relativity, there are two sets of PDEs: Evolution equations and constraints which are preserved in time. As in the classical theory, it is simplest to fix the gauge and write these equations using the advanced and retarded coordinates z^\pm of the fiducial Minkowski metric. The evolution equations are given by

$$\square_{(\eta)} f^{(i)} = 0 \quad \Leftrightarrow \quad \square_{(g)} f^{(i)} = 0. \quad (2.1)$$

for matter fields and

$$\begin{aligned} \partial_+ \partial_- \Phi + \kappa^2 \Theta &= G \langle \hat{T}_{+-} \rangle \equiv \bar{N} G \hbar \partial_+ \partial_- \ln \Phi \Theta^{-1} \\ \Phi \partial_+ \partial_- \ln \Theta &= -G \langle \hat{T}_{+-} \rangle \equiv -\bar{N} G \hbar \partial_+ \partial_- \ln \Phi \Theta^{-1} \end{aligned} \quad (2.2)$$

for the geometrical fields where, as before, $\bar{N} = N/24$. The constraint equations tie the geometrical fields Θ, Φ to the matter fields f_i . They are preserved in time. Therefore we can

impose them just at \mathcal{I}^- where they take the form:

$$-\partial_-^2 \Phi + \partial_- \Phi \partial_- \ln \Theta = G \langle \hat{T}_{--} \rangle \doteq 0 \quad (2.4)$$

and

$$-\partial_+^2 \Phi + \partial_+ \Phi \partial_+ \ln \Theta = G \langle \hat{T}_{++} \rangle \doteq 12 \bar{N} G (\partial_+ f_+^o)^2 \quad (2.5)$$

where \doteq stands for ‘equality at \mathcal{I}^- ’.

We will conclude this discussion of the field equations with a few remarks, and a description of our initial conditions. Because $\hat{f}_-^{(i)}$ are all in the vacuum state, it follows immediately that, as in the classical theory, all the right moving fields vanish; $f_-^{(i)} = 0$ also in the mean-field theory. Similarly, because $\hat{f}_+^{(i)}$ are in a coherent state peaked at some classical profile f_+^o , it follows that, for all i , $f_+^{(i)}(z^+) = f_+^o(z^+)$ (on the entire fiducial Minkowski manifold M^o). Thus, as far as matter fields are concerned, there is no difference between the classical and mean-field theory. Similarly, as in the classical theory, we can integrate the constraint equations to obtain initial data on two null hypersurfaces. We will assume that $f_+^{(o)}$ vanishes to the past of the line $z^+ = z_o^+$. Let I_L^- denote the line $z^+ = z_o^+$ and I_R^- the portion of the line $z^- = z_o^- \ll -1/\kappa$ to the future of $z^+ = z_o^+$. We will specify initial data on these two surfaces. The solution to the constraint equations along these lines is not unique and, as in the classical theory we require additional physical input to select one. We will again require that Φ be in the dilaton vacuum to the past of I_L^- and by continuity on I_L^- . Following the CGHS literature, we will take it to be $\Phi = e^{\kappa(z^+ - z^-)}$.⁵ Thus, the initial values of semi-classical Θ, Φ coincide with those of classical $\underline{\Theta}, \underline{\Phi}$:

$$\Theta \doteq e^{\kappa(z_o^+ - z^-)} \quad \text{on all of } I_L^- \text{ and } I_R^- \quad (2.6)$$

and

$$\begin{aligned} \Phi &\doteq \Theta \quad \text{on } I_L^- \text{ and,} \\ \Phi &\doteq \Theta - 12 \bar{N} G \int_{-\infty}^{z^+} d\bar{z}^+ e^{\kappa \bar{z}^+} \int_{-\infty}^{\bar{z}^+} d\bar{z}^- e^{-\kappa \bar{z}^-} \left(\frac{\partial f_+^{(o)}}{\partial \bar{z}^-} \right)^2 \\ &\quad \text{on } I_R^- \end{aligned} \quad (2.7)$$

(see (1.7)). The difference in the classical and semi-classical theories lies entirely in the evolution equations (2.2) and (2.3). In the classical theory, the right hand sides of these equations vanish whence one can easily integrate them. In the mean-field theory, this is not possible and one has to take recourse to numerical methods. Finally, while our analytical considerations hold for any regular profile f_+^o , to begin with we will follow the CGHS literature in Sec. III A and Sec. III B and specify f_+^o to represent a collapsing shell:

$$12 \bar{N} \left(\frac{\partial f_+^o}{\partial z^+} \right)^2 = M_{\text{ADM}} \delta(z^+) \quad (2.8)$$

⁵ Strictly, since $\hat{\Phi}$ is an operator on the tensor product of N Fock spaces, one for each $\hat{f}^{(i)}$, the expectation value is $N e^{\kappa(z^+ - z^-)}$. But this difference can be compensated by shifting z^- . We have chosen to use the convention in the literature so as to make translation between our expressions and those in other papers easier.

so the shell is concentrated at $z^+ = 0$. In the literature this profile is often expressed, using x^+ in place of z^+ , as:

$$12\bar{N} \left(\frac{\partial \tilde{f}_+^o}{\partial x^+} \right)^2 = M_{\text{ADM}} \delta(x^+ - \frac{1}{\kappa}) \quad (2.9)$$

where $\tilde{f}^{(o)}(x^+) = f^{(o)}(z^+)$. In Sec. IIIC we will discuss results from a class of smooth matter profiles.

B. Singularity, horizons and the Bondi mass

The classical solution (1.7) has a singularity ℓ_s where Φ vanishes. As remarked in section I, in the mean-field theory, a singularity persists but it is shifted to $\Phi = 2\bar{N}G\hbar$ [2]. The metric $g^{ab} = \Theta^{-1}\Phi\eta^{ab}$ is invertible and continuous there but not C^1 . Thus the singularity is weakened relative to the classical theory. Furthermore, its spatial extension is diminished. As indicated in Fig.2, the singularity now originates at a finite point on the collapsing shell (i.e. does not extend to \mathcal{I}_L^+) and it ends in the space-time interior (i.e., does not extend to \mathcal{I}_R^+).

What is the situation with horizons? Recall from section I that, in the spherically symmetric reduction from 4-dimensions, $r^2 = e^{-2\phi}/\kappa^2 := \Phi/\kappa^2$ and each round 2-sphere in 4-dimensional space-time projects down to a single point on the 2-manifold M . Thus, in the CGHS model we can think of Φ as defining the ‘area’ associated with any point. (It is dimensionless because in D space-time dimensions the area of spatial spheres has dimensions $[L]^{D-2}$.) Therefore it is natural to define a notion of trapped points: A point in the CGHS space-time (M, g) is said to be *future trapped* if $\partial_+\Phi$ and $\partial_-\Phi$ are both negative there and *future marginally trapped* if $\partial_+\Phi$ vanishes and $\partial_-\Phi$ is negative there [2, 15]. In the classical solution resulting from the collapse of a shell (2.8), all the marginally trapped points lie on the event horizon and their area is a constant; we only encounter an isolated horizon [16] (see Fig.1). The mean-field theory is much richer because it incorporates the back reaction of quantum radiation. In the case of a shell collapse, the field equations now imply that a marginally trapped point first forms at a point on the shell and has area

$$\begin{aligned} \mathbf{a}_{\text{initial}} &:= (\Phi - 2\bar{N}G\hbar)|_{\text{initial}} \\ &= -\bar{N}G\hbar + \bar{N}G\hbar \left(1 + \frac{M_{\text{ADM}}^2}{\bar{N}^2\hbar^2\kappa^2} \right)^{\frac{1}{2}} \end{aligned} \quad (2.10)$$

As time evolves, this area *shrinks* because of quantum radiation [2]. The world-line of these marginally trapped points forms a *generalized dynamical horizon* (GDH), ‘generalized’ because the world-line is time-like rather than space-like [16]. (In 4 dimensions these are called marginally trapped tubes [17].) The area finally shrinks to zero. This is the point at which the GDH meets the end-point of the (weak) singularity [2, 12, 18] (see Fig.2). It is remarkable that all these interesting dynamics occur simply because, unlike in the classical theory, the right sides of the dynamical equations (2.2), (2.3) are non-zero, given by the trace-anomaly.

We will see in section III that while the solution is indeed asymptotically flat at \mathcal{I}_R^+ , in contrast to the classical solution, \mathcal{I}_R^+ is *no longer complete*. More precisely, the space-time (M, g) now has a future boundary at the last ray—the null line to \mathcal{I}_R^+ from the point at which the singularity ends—and the affine parameter along \mathcal{I}_R^+ with respect to g_{ab} has a *finite value* at the point where the last ray meets \mathcal{I}_R^+ . Therefore, in the semi-classical theory, we *cannot even ask if this space-time admits an event horizon*. While the notion of an event horizon is global and teleological, the notion of trapped surfaces and GDHs is quasi-local. As we have just argued, these continue to be meaningful in the semi-classical theory. What forms and evaporates is the GDH.

Next, let us discuss the structure at null infinity [7, 8]. As in the classical theory, we assume that the semi-classical space-time is asymptotically flat at \mathcal{I}_R^+ in the sense that, as one takes the limit $z^+ \rightarrow \infty$ along the lines $z^- = \text{const}$, the fields Φ, Θ have the following behavior:

$$\begin{aligned} \Phi &= A(z^-) e^{\kappa z^+} + B(z^-) + O(e^{-\kappa z^+}) \\ \Theta &= \underline{A}(z^-) e^{\kappa z^+} + \underline{B}(z^-) + O(e^{-\kappa z^+}), \end{aligned} \quad (2.11)$$

where $A, B, \underline{A}, \underline{B}$ are some smooth functions of z^- . Note that the leading order behavior in (2.11) is the same as that in the classical solution. The only difference is that B, \underline{B} are not required to be constant along \mathcal{I}_R^+ because, in contrast to its classical counterpart, the semi-classical space-time is non-stationary near null infinity due to quantum radiation. Therefore, as in the classical theory, \mathcal{I}_R^+ can be obtained by taking the limit $z^+ \rightarrow \infty$ along the lines $z^- = \text{const}$. The asymptotic conditions (2.11) on Θ, Φ imply that curvature—i.e., the Ricci scalar of g_{ab} —goes to zero at \mathcal{I}_R^+ . We will see in section III that these conditions are indeed satisfied in semi-classical space-times that result from collapse of matter from \mathcal{I}_R^- .

Given this asymptotic fall-off, the field equations determine \underline{A} and \underline{B} in terms of A and B . The metric g_{ab} admits an *asymptotic* time translation t^a which is unique up to a constant rescaling and the rescaling freedom can be eliminated by requiring that it be (asymptotically) unit. The function $A(z^-)$ determines the affine parameter y^- of t^a via:

$$e^{-\kappa y^-} = A(z^-). \quad (2.12)$$

Thus y^- can be regarded as the unique asymptotic time parameter with respect to g_{ab} (up to an additive constant). Near \mathcal{I}_R^+ the mean-field metric g can be expanded as:

$$dS^2 = - \left(1 + B e^{\kappa(y^- - y^+)} + O(e^{-2\kappa y^+}) \right) dy^+ dy^- \quad (2.13)$$

where $y^+ = z^+$.

Finally, equations of the mean-field theory imply [7, 8] that there is a balance law at \mathcal{I}_R^+ :

$$\begin{aligned} \frac{d}{dy^-} \left[\frac{dB}{dy^-} + \kappa B + \bar{N}\hbar G \left(\frac{d^2 y^-}{dz^{-2}} \left(\frac{dy^-}{dz^-} \right)^{-2} \right) \right] \\ = - \frac{\bar{N}\hbar G}{2} \left[\frac{d^2 y^-}{dz^{-2}} \left(\frac{dy^-}{dz^-} \right)^{-2} \right]^2. \end{aligned} \quad (2.14)$$

In [7], this balance law was used to introduce a new notion of Bondi mass and flux. The left side of (2.14) led to the definition of the Bondi mass:

$$M_{\text{Bondi}}^{\text{ATV}} = \frac{dB}{dy^-} + \kappa B + \bar{N} \hbar G \left(\frac{d^2 y^-}{dz^{-2}} \left(\frac{dy^-}{dz^-} \right)^{-2} \right), \quad (2.15)$$

while the right side provided the Bondi flux:

$$F^{\text{ATV}} = \frac{\bar{N} \hbar G}{2} \left[\frac{d^2 y^-}{dz^{-2}} \left(\frac{dy^-}{dz^-} \right)^{-2} \right]^2, \quad (2.16)$$

so that we have:

$$\frac{dM_{\text{Bondi}}^{\text{ATV}}}{dy^-} = -F^{\text{ATV}}. \quad (2.17)$$

By construction, as in 4 dimensions, the flux is manifestly positive so that $M_{\text{Bondi}}^{\text{ATV}}$ decreases in time. Furthermore, it vanishes on an open region if and only if $y^- = C_1 z^- + C_2$ for some constants C_1, C_2 , i.e. if and only if the asymptotic time translations defined by the physical, mean field metric g and by the fiducial metric η agree at \mathcal{I}_R^+ , or, equivalently, if and only if the asymptotic time translations of g on \mathcal{I}_L^- and \mathcal{I}_R^+ agree. Finally, note that $g^{ab} = \eta^{ab}$, $f_{\pm} = 0$, $\Phi = \Theta = \exp \kappa(z^+ - z^-)$, is a solution to the full mean-field equations. As one would expect, both $M_{\text{Bondi}}^{\text{ATV}}$ and F^{ATV} vanish for this solution.

The balance law is just a statement of conservation of energy. As one would expect, \hbar appears as an overall multiplicative constant in (2.16); in the classical theory, there is no flux of energy at \mathcal{I}_R^+ . If we set $\hbar = 0$, $M_{\text{Bondi}}^{\text{ATV}}$ reduces to the standard Bondi mass formula in the classical theory (see e.g., [15]). Previous literature [1, 2, 14, 15, 18–20] on the CGHS model used this classical expression also in the semi-classical theory. Thus, in the notation we have introduced here, the traditional definitions of mass and flux are given by

$$M_{\text{Bondi}}^{\text{Trad}} = \frac{dB}{dy^-} + \kappa B, \quad (2.18)$$

and

$$F^{\text{Trad}} = F^{\text{ATV}} + \bar{N} \hbar G \frac{d}{dy^-} \left(\frac{d^2 y^-}{dz^{-2}} \left(\frac{dy^-}{dz^-} \right)^{-2} \right). \quad (2.19)$$

As noted in section I, numerical simulations have shown that $M_{\text{Bondi}}^{\text{Trad}}$ can become negative and large even when the horizon area is large, while $M_{\text{Bondi}}^{\text{ATV}}$ remains positive throughout the evaporation process.

C. Scaling and the Planck regime

Finally, we note a scaling property of the mean-field theory, which Ori recently and independently also uncovered [11] and which is also observed in other quantum gravitational systems [21]. We were led to it while attempting to interpret numerical results which at first seemed very puzzling; it is thus a concrete example of the how useful the interplay between numerical and analytical studies can be. Let us fix z^{\pm}

and regard all fields as functions of z^{\pm} . Consider any solution $(\Theta, \Phi, N, f_+^{(i)})$ to our field equations, satisfying boundary conditions (2.6) and (2.7). Then, given a positive number λ , $(\tilde{\Theta}, \tilde{\Phi}, \tilde{N}, \tilde{f}_+^{(i)})$ given by⁶

$$\tilde{\Theta}(z^+, z^-) = \lambda \Theta(z^+, z^- + \frac{\ln \lambda}{\kappa}), \quad \tilde{N} = \lambda N$$

$$\tilde{\Phi}(z^+, z^-) = \lambda \Phi(z^+, z^- + \frac{\ln \lambda}{\kappa}), \quad \tilde{f}_+^{(i)}(z^+) = f_+^{(i)}(z^+)$$

is also a solution satisfying our boundary conditions, where, as before, we have assumed that all scalar fields have an identical profile f_+^o . Note that f_+^o is completely general; we have not restricted ourselves, e.g., to shells. Under this transformation, we have

$$\begin{aligned} \bar{g}^{ab} &\rightarrow \bar{g}^{ab} \\ y^- &\rightarrow y^- - \frac{1}{\kappa} \ln \lambda \\ M_{\text{ADM}} &\rightarrow \lambda M_{\text{ADM}} \\ M_{\text{Bondi}}^{\text{ATV}} &\rightarrow \lambda M_{\text{Bondi}}^{\text{ATV}} \\ F^{\text{ATV}} &\rightarrow \lambda F^{\text{ATV}} \\ \mathbf{a}_{\text{GDH}} &\rightarrow \lambda \mathbf{a}_{\text{GDH}} \end{aligned} \quad (2.20)$$

where \mathbf{a}_{GDH} denotes the area of the generalized dynamical horizon. This symmetry implies that, *as far as space-time geometry and energetics are concerned, only the ratios M/N matter, not separate values of M and N themselves* (where M can either be the ADM or the Bondi mass). Thus, for example, whether for the evaporation process a black hole is ‘macroscopic’ or ‘Planck size’ depends on the ratios M/N and $\mathbf{a}_{\text{GDH}}/N$ rather than on the values of M or \mathbf{a}_{GDH} themselves.

We will set

$$\begin{aligned} M^* &= M_{\text{ADM}}/\bar{N} \\ M_{\text{Bondi}}^* &= M_{\text{Bondi}}^{\text{ATV}}/\bar{N}, \text{ and} \\ m^* &= M_{\text{Bondi}}^*|_{\text{last ray}} \end{aligned} \quad (2.21)$$

(We use $\bar{N} = N/24$ in these definitions because the dynamical equations feature \bar{N} rather than N .) We will need to compare these quantities with the Planck mass. Now, in 2 dimensions, G , \hbar and c do not suffice to determine Planck mass, Planck length and Planck time uniquely because $G\hbar$ is dimensionless. But in 4 dimensions we have unambiguous definitions of these quantities and, conceptually, we can regard the 2 dimensional theory as obtained by its spherical reduction. In 4-dimensions, (using the $c=1$ units used here) the Planck mass is given by $M_{\text{Pl}}^2 = \hbar/G_4$ and the Planck time by $\tau_{\text{Pl}}^2 = G_4 \hbar$. From Eqs (1.2) and (1.3) it follows that G_4 is related to the 2-dimensional Newton’s constant G via $G = G_4 \kappa^2$. Therefore we are led to set

$$M_{\text{Pl}}^2 = \frac{\hbar \kappa^2}{G}, \quad \text{and} \quad \tau_{\text{Pl}}^2 = \frac{G \hbar}{\kappa^2}. \quad (2.22)$$

⁶ The shift in z^- is needed because we chose to use the initial value $\Theta = e^{\kappa(z^+ - z^-)}$ on \mathcal{I}_L^- as in the literature rather than $\Theta = N e^{\kappa(z^+ - z^-)}$. See footnote 5.

When can we say that a black hole is macroscopic? One's first instinct would be to say that the ADM mass should be much larger than M_{Pl} in (2.22). But this is not adequate for the evaporation process because the process depends also on the number of fields N . In the external field approximation where one ignores the back reaction, we know that at late times the black hole radiates as a black body at a fixed temperature $T_{\text{Haw}} = \kappa\hbar$.⁷ The Hawking energy flux at \mathcal{I}_R^+ is given by $F^{\text{Haw}} = \bar{N}\kappa^2\hbar/2$. Therefore the evaporation process will last much longer than 1 Planck time if and only if $(M_{\text{ADM}}/F^{\text{Haw}}) \gg \tau_{\text{Pl}}$, or, equivalently

$$M^* \gg G\hbar M_{\text{Pl}}. \quad (2.23)$$

(Recall that $G\hbar$ is the Planck number.) So, a necessary condition for a black hole to be macroscopic is that M^* should satisfy this inequality. In section III we will see that, in the mean-field theory, quantum evaporation reveals universality already if $M^* \gtrsim 4G\hbar M_{\text{Pl}}$.

III. ANTICIPATED AND UNFORESEEN BEHAVIOR

All physical predictions of the mean-field theory arise from the set of 5 equations (2.1) – (2.5). The only difference from the classical theory lies in the fact that, because of the trace anomaly, right hand sides of the dynamical equations (2.2) and (2.3) are no longer zero. But this difference has very significant ramifications. In particular, it is no longer possible to obtain explicit analytical solutions; one has to take recourse to numerics.⁸

Also, we now have interesting time-dependent phenomena such as formation and evaporation of dynamical horizons. Given these differences, a number of global questions naturally arise. Does the space-time continue to be asymptotically flat at \mathcal{I}_R^+ in the mean-field theory? If so, is \mathcal{I}_R^+ complete as in the classical theory? Is the Bondi mass positive? Does it go to the Planck scale as the horizon area goes to zero? Is the flux of energy of the quantum radiation constant, given by $\hbar\kappa^2\bar{N}/2$ at late times, as in the external field approximation *a la* Hawking [25, 26]? If not, the quantum radiation would

not be compatible with thermal flux, violating a key assumption that has been made over the years.

Recall from section II B that since our profile functions $f_+^{(o)}$ vanish to the past of a null ray I_L^- , the solution in the past is given by $f^{(i)} = 0$, $g_{ab} = \eta_{ab}$, $\Theta = \Phi = e^{\kappa(z^+ - z^-)}$. To obtain it to the future of I_L^- , we use the initial data on I_L^- and I_R^- given by (2.6) and (2.7). The dynamical equations (2.1), (2.2) are hyperbolic and therefore well adapted to numerical evolution. They have been solved numerically before (see, in particular, [12, 18–20]), and much information has been learnt about the CGHS model, for example the dynamics of the GDH and that it evaporates to zero area, terminating in a naked singularity. However, to our knowledge in all these simulations, the choice of parameters M_{ADM} and N was such that $M^* = M_{\text{ADM}}/\bar{N}$ was less than 2.5. As we will see, in a precise sense, these black holes are Planck scale already when they are formed.

Reliable simulations of macroscopic black holes with $M^* \gtrsim 5 - 10$ turn out to be much harder to perform, and several additional steps beyond a straight-forward discretization are necessary to study this regime [9]. First, one needs to formulate the problem in terms of ‘regularized’ variables which do not diverge at infinity. Second, one needs to introduce coordinates which (a) bring the infinite portion of \mathcal{I}_R^+ of interest to a compact interval, and (b) enlarge the region near the last ray by a factor of roughly e^{M^*} relative to a uniform discretization of the (compactified) time-translation coordinate z^- . (In other words, a region in the vacuum solution near I_L^- of physical size equal to $\sim e^{-M^*}$ expands to a region of physical size $O(1)$ on \mathcal{I}_R^+ , where all the interesting dynamics occurs.) Third, to achieve this latter part of the coordinate transformation one needs to know the location of the last ray extremely well, requiring high accuracy numerical methods. This is achieved by using Richardson extrapolation with intermittent error removal, beginning with a unigrid method that is second order accurate. With four successively finer meshes the overall rate of convergence of the scheme is $\mathcal{O}(h^7)$, and this was sufficient to reduce the truncation error to the order of machine round-off ($\sim 10^{-16}$). These high precision numerical calculations showed that, while some of the long held assumptions on the nature of quantum evaporation are borne out, several are not. We summarize these results from a physical perspective in the next three sub-sections. Complementary discussion of numerical issues appears in [9].

Numerical calculations were performed for a range of rescaled ADM masses M^* from 2^{-10} to 16 and N varying from 12 to 24000. Since in this paper we are primarily interested in black holes which are initially macroscopic, we will focus on $M^* \geq 1$ and, since our simulations exhibited the expected scaling behavior, all our plots, except Fig. 5, are for $N = 24$ (i.e., $\bar{N} = 1$). Finally, in these simulations we set $\hbar = G = \kappa = 1$. The first two sub-sections summarize results from a shell collapse and the third sub-section reports on results obtained from more general infalling profiles.

⁷ Note that this relation is the same as that in 4 dimensions because the classical CGHS black hole is stationary to the future of the collapsing matter with surface gravity κ . However, there is also a *key* difference: now κ is just a constant, independent of the mass of the black hole. Therefore, unlike in 4-dimensions, the temperature of the CGHS black hole is a universal constant in the external field approximation. Therefore, when back reaction is included, one does not expect a CGHS black hole to get hotter as it shrinks.

⁸ There are variants of the CGHS model that are explicitly soluble, for example the RST (Russo-Susskind-Thorlacius) model [22], and the Bilal-Callan model [23]. However, results obtained in these models are not likely to be generic even in 2 dimensions because of their extra symmetries [12, 20]. More importantly, it was pointed out in [2, 12, 24] that the RST model is inconsistent even in the large N limit, and the Bilal-Callan model has a Hamiltonian that is unbounded from below. Thus though they exhibit many features of general 2D semi-classical black hole evaporation, they are physically less interesting than the CGHS model.

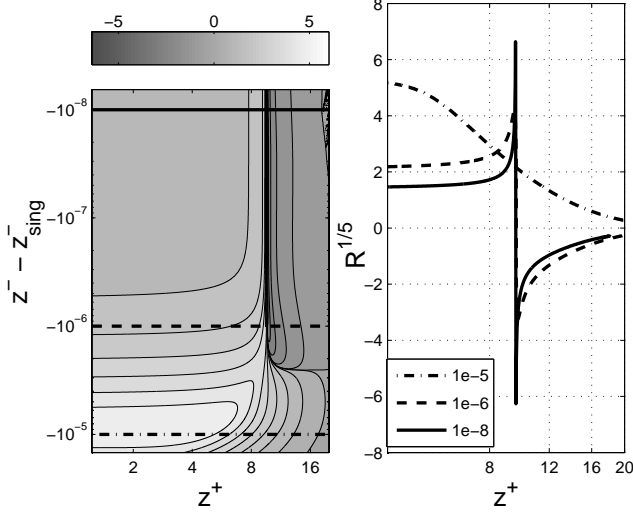


Figure 3. The Ricci scalar R for $M^* = 8$. Left: 2D contour plot of $R^{1/5}$ showing the increase in R as the singularity (dark vertical region near the middle) is approached and the asymptotically flat region ($R \rightarrow 0$) near \mathcal{I}_R^+ ($z^+ \rightarrow \infty$). Right: $R^{1/5}$ as a function of z^+ on the lines $z^- - z_{\text{sing}}^- = -10^{-5}, -10^{-6}, -10^{-8}$ (marked on the left panel as horizontal lines), showing a double peak, indicating the divergent behavior of $\partial_+ \partial_- \Phi$ at the singularity. The fact that the peak is narrow rules out a strong thunderbolt singularity. Note that the dark color at the region of the singularity is due to the high density of contour lines, and not directly due to negative values of R . While naive numerical calculation of R very close to \mathcal{I}_R^+ does not yield reliable results due to catastrophic cancellation, it is already very small in the high z^+ values shown here, and the trend towards 0 is clear.

A. Shell Collapse: Anticipated Behavior

Asymptotic flatness at \mathcal{I}_R^+ : First, Θ, Φ do indeed satisfy the asymptotic conditions (2.11). This was also noted in the recent approximate solution to the CGHS equations by Ori [11]. The simulations provide values of the functions $A(z^-), B(z^-)$ and $y^-(z^-)$. As a consistency check on the simulation, we verified the balance law (2.14) by calculating separately the right and left sides of this equation as close to the last ray as the numerical solution gave reliable (convergent) results. We also computed the scalar curvature R of the mean-field metric g , and it does go to zero at \mathcal{I}_R^+ —see Fig. 3 for an example.

Finiteness of y^- at the last ray: In the classical solution, the affine parameters \underline{y}^- along \mathcal{I}_R^+ and z^- along \mathcal{I}_L^- defined by \underline{g} are related by

$$e^{-\kappa \underline{y}^-} = e^{-\kappa z^-} - \frac{GM}{\kappa}. \quad (3.1)$$

Hence $\underline{y}^- = \infty$ at $\kappa z^- = -\ln(GM/\kappa)$. This is the point at which the singularity and the event horizon meet \mathcal{I}_R^+ (see Fig 1). Thus, in the classical solution \mathcal{I}_R^+ is complete but, in a precise sense, smaller than \mathcal{I}_L^- . For a test quantum field \hat{f}_- on the classical solution, one then has to trace over modes

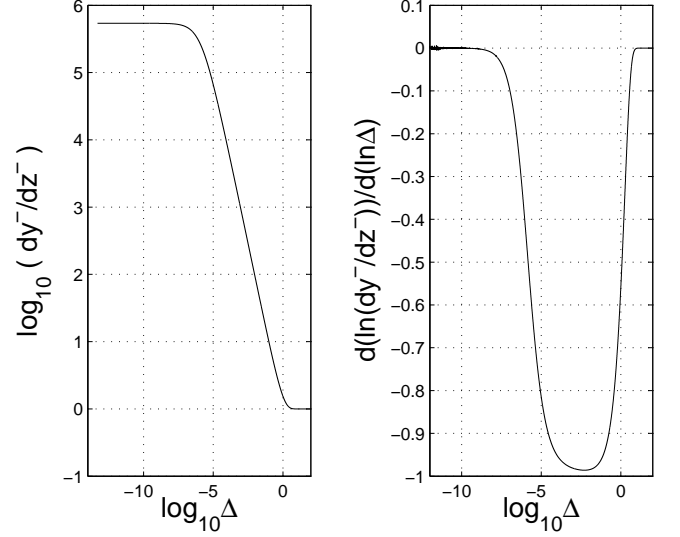


Figure 4. Left: Plot of $\log_{10}(dy^-/dz^-)$ vs $\log_{10} \Delta$ for $M^* = 8$, $\bar{N} = 1$, where $\Delta = (z_{\text{sing}}^- - z^-)$. Right: Slope of the curve on the left. If locally the function on the left behaves as $\sim (\kappa \Delta)^{-p}$, the curve on the right shows $-p$. In the distant past (rightmost region in both plots), y^- tends to z^- . The intermediate region is similar to that in the classical solution where $(dy^-/dz^-) \sim (\kappa \Delta)^{-1}$. As the last ray is further approached (leftmost region), we see that (dy^-/dz^-) increases much slower than $(\kappa \Delta)^{-1}$, leading to a finite value for y^- at the last ray.

residing on the part of \mathcal{I}_L^- which is missing from \mathcal{I}_R^+ . This fact is directly responsible for pure states on \mathcal{I}_L^- to evolve to mixed states on \mathcal{I}_R^+ , i.e., for the non-unitarity of the S -matrix [7, 8] of the test field. What is the situation in the mean-field theory? Our analysis shows that, as generally expected, the affine parameter w.r.t. the mean field metric g takes a *finite* value at the last ray on \mathcal{I}_R^+ ; a necessary condition for unitarity of the S -matrix is met.

To establish this result, we apply the following strategy. Let us return to the classical solution \underline{g} and set

$$\kappa z_{\text{sing,cl}}^- = -\ln(GM/\kappa) \quad \text{and} \quad \Delta_{\text{cl}} = z_{\text{sing,cl}}^- - z^-. \quad (3.2)$$

(The subscript ‘sing,cl’ just highlights the fact that this is the point at which the classical singularity meets \mathcal{I}_R^+ .) Then we have

$$\underline{y}^- = z^- - \frac{1}{\kappa} \ln(1 - e^{-\kappa \Delta_{\text{cl}}}). \quad (3.3)$$

When Δ_{cl} tends to zero, \underline{y}^- is dominated by the leading order term $-(1/\kappa) \ln(-\kappa \Delta_{\text{cl}})$ which diverges at $\Delta_{\text{cl}} = 0$. This logarithmic divergence is coded in the power -1 in the expression of the derivative $(d\underline{y}^-/dz^-)$:

$$\frac{d\underline{y}^-}{dz^-} = (\kappa \Delta_{\text{cl}})^{-1} + \text{finite terms}. \quad (3.4)$$

If we had $(\kappa \Delta_{\text{cl}})^{-p}$ on the right side rather than $(\kappa \Delta_{\text{cl}})^{-1}$, then \underline{y}^- would have been finite at the future end of \mathcal{I}_R^+ of \underline{g} for $p < 1$ (as then $\underline{y}^- = (\kappa \Delta_{\text{cl}})^{1-p}/(1-p) + \text{finite terms}$).

In the mean-field theory, the last ray starts at the end point of the singularity and meets \mathcal{I}_R^+ of g at its future end point. We will denote it by the line $z^- = z_{\text{sing}}^-$. Following the above discussion, to show that the affine parameter y^- w.r.t. g is finite at $z^- = z_{\text{sing}}^-$ we focus on the behavior of (dy^-/dz^-) near this future end point of \mathcal{I}_R^+ . More precisely, we analyze the functional behavior of (dy^-/dz^-) and determine a local p extracted from the logarithmic derivative of (dy^-/dz^-) with respect to $\Delta \equiv z_{\text{sing}}^- - z^-$. Results in Fig. 4 show that (dy^-/dz^-) grows much slower near the last ray in the mean-field theory than it does in the classical theory. In fact, over the entire range of \mathcal{I}_R^+ the local estimate of p is strictly less than 1, and asymptotes to 0 approaching the last ray. This implies that y^- is finite at the last ray in the mean-field theory.

Note that the above analysis is only valid if we have determined the location of the singularity with sufficient accuracy such that the numerical uncertainty in its location is much smaller than the range in Δ where we extract the asymptotic behavior of the function. From convergence studies we estimate our precision in determining z_{sing}^- is at the order of 10^{-13} , and hence all the values in Fig. 4 are sufficiently far from the last ray to provide a reliable measure of the power p .

B. Shell collapse: Unforeseen Behavior

The numerical calculations also revealed a number of surprises which we now discuss.

Bondi mass for large \bar{N} : Scaling properties discussed in section II imply that if the Bondi mass at the last ray is finite, it will be macroscopic for a sufficiently large N . This expectation is borne out (in particular the Bondi mass *is* finite) in all our simulations with large M_{ADM} and large \bar{N} . Fig. 5 summarizes the result of a simulation where $N = 720$ and $M_{\text{ADM}} = 360$ (so $\bar{N} = 30$ and $M^* = 12$). The Bondi mass, $M_{\text{Bondi}}^{\text{Trad}}$, that has been commonly used in the literature [1, 2, 14, 15, 18–20] becomes negative even far from the last ray when the horizon area is still macroscopic, and has a macroscopic negative value at the last ray.⁹ On the other hand, the more recent $M_{\text{Bondi}}^{\text{ATV}}$ [7, 8] remains strictly positive. As one would expect from the scaling relations, because N is large, $M_{\text{Bondi}}^{\text{ATV}}$ is also macroscopic at the last ray.

Universality of the end state: Fig 6 shows a plot of m^* , the value of $(M_{\text{Bondi}}^{\text{ATV}}/\bar{N})$ at the last ray, against $M^* = (M_{\text{ADM}}/\bar{N})$, for several values of the initial $M^* > 1$. The curve that fits the data, shown in the figure, is

$$m^* = \alpha (1 - e^{-\beta(M^*)^\gamma}) \quad (3.5)$$

with specific values for the constants α, β, γ

$$\alpha \approx 0.864, \quad \beta \approx 1.42, \quad \gamma \approx 1.15.$$

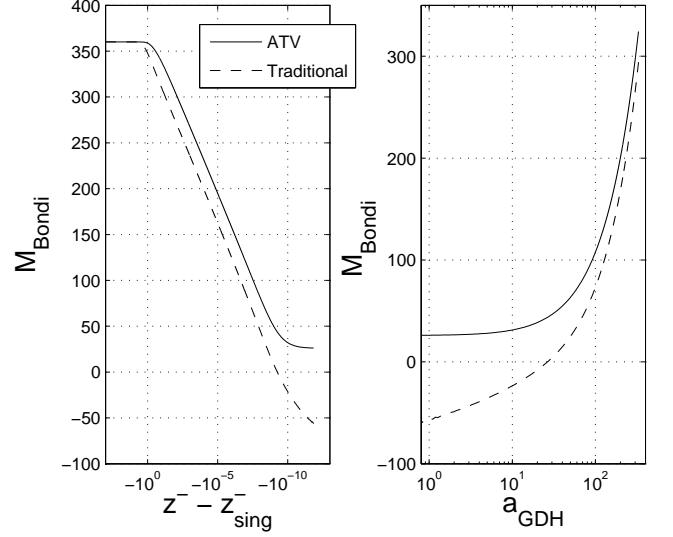


Figure 5. The ATV Bondi mass $M_{\text{Bondi}}^{\text{ATV}}$ (solid lines) and the traditional Bondi mass $M_{\text{Bondi}}^{\text{Trad}}$ (dashed lines) are plotted against $z^- - z_{\text{sing}}^-$ (left) and the horizon area (right). This simulation corresponds to $M_{\text{ADM}} = 360$, $N = 720$ (so $M^* = 12$). For high values of N , both formulas give a large non-zero Bondi mass at the last ray. $M_{\text{Bondi}}^{\text{Trad}}$ becomes negative when the area is still macroscopic. On the other hand $M_{\text{Bondi}}^{\text{ATV}}$ remains strictly positive all the way to the last ray, where the generalized dynamical horizon (GDH) shrinks to zero area.

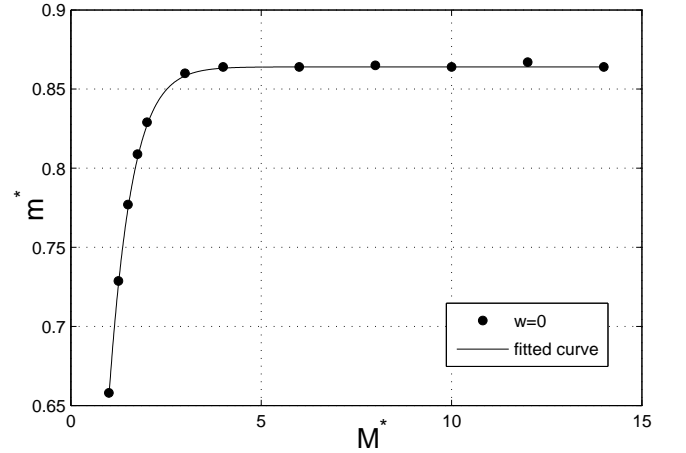


Figure 6. The value of m^* (i.e. $M_{\text{Bondi}}^{\text{ATV}}/\bar{N}$ at the last ray) is plotted against M^* (which equals M_{ADM}/\bar{N}) for $M^* \geq 1$. For Macroscopic M^* (actually, already for $M^* \gtrsim 4$!) m^* has a universal value, approximately 0.864.

It is visually clear from the plot that there is a qualitative difference between $M^* \gtrsim 4$ and $M^* \lesssim 4$. Physically this can be understood in terms of a_{initial}^* , the area of the first marginally trapped surface: Eq (2.10) implies that $a_{\text{initial}}^* = a_{\text{initial}}/\bar{N}$ can be greater than a Planck unit only if M^* is larger than 3. It is therefore not surprising that $M^* = 4$ should serve as

⁹ After this work was completed, Javad Taghizadeh Firouzjaee pointed out to us that the fact that the traditional Bondi mass can become negative was already noticed in [19]. Again though, in our terminology the numerical simulation in that work corresponds to a microscopic black hole with $M^* = 1 M_{\text{Pl}}$.

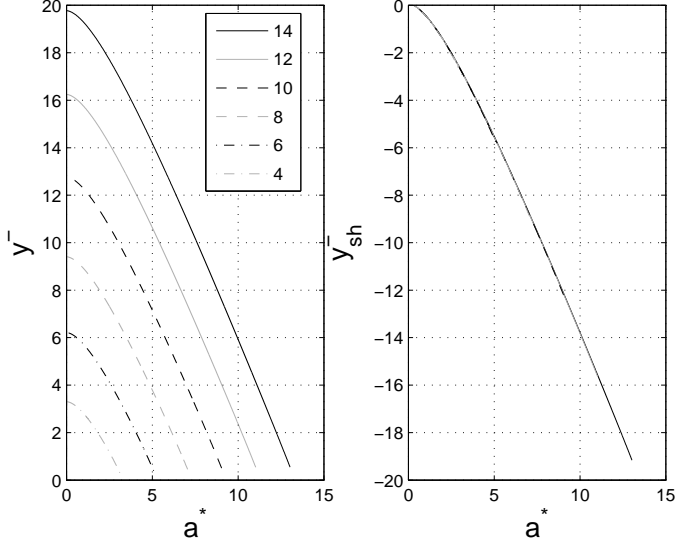


Figure 7. Left: The affine parameter y^- (defined in Eq. (2.12) of the physical metric g is plotted against the rescaled area $\mathbf{a}^* := (\mathbf{a}_{\text{GDH}}/\bar{N})$ of the generalized dynamical horizon (given by $(\Phi/\bar{N} - 2)$) at the horizon for values of M^* from 4 to 14. Even though the curves are very similar in shape, they do not coincide. Right: Once the shifting freedom in y^- is utilized, we see that a properly shifted version y_{sh}^- is universal with respect to \mathbf{a}^* for all macroscopic M^* values. y_{sh}^- can be used as a universal coordinate similar to the horizon area.

the boundary between macro and Planck regimes. Indeed, as Fig 6 shows, if $M^* \gtrsim 4$, the value of the end point Bondi mass is universal, $m^* \approx 0.864$. For $M^* \lesssim 4$ on the other hand, the value of m^* depends sensitively on M^* . This could have been anticipated because if $M^* \leq 3$, what evaporates is a GDH which *starts out* with one Planck unit or less of area \mathbf{a}^* . Thus, in the mean-field approximation it is natural to regard CGHS black holes with $M^* \gtrsim 4$ as macroscopic and those with $M^* \lesssim 4$ as microscopic. Finally, for macroscopic black holes, the end-value of the traditional Bondi-mass is also universal: $M_{\text{Bondi}}^{\text{Trad}} < \mathbf{a}_{\text{hor}}$ and $(M_{\text{Bondi}}^{\text{Trad}}/\bar{N}) \rightarrow -2.0$ as $\mathbf{a}_{\text{hor}} \rightarrow 0$.

As noted in the beginning of section III, there have been a number of previous numerical studies of the CGHS model [12, 18–20]. They clarified several important dynamical issues. However they could not unravel universality because they all focused on cases where the black hole is microscopic already at its inception: $M^* \leq 2.5$ in [18], $M^* = 1$ in [12] and [19] and $M^* = 0.72$ in [20]. This limitation was not noticed because the scaling symmetry and its significance was not appreciated.

Dynamical universality of y^- : The horizon area \mathbf{a}_{GDH} (more precisely, its negative) provides an invariantly defined time coordinate to test dynamical universality of other physical quantities. Let us begin with y^- , the affine parameter along \mathcal{I}_R^+ with respect to the physical metric g defined in (2.12). Fig. 7, left, shows the plot of y^- against $\mathbf{a}^* := (\mathbf{a}_{\text{GDH}}/\bar{N})$ for various values of M^* . These plots show that

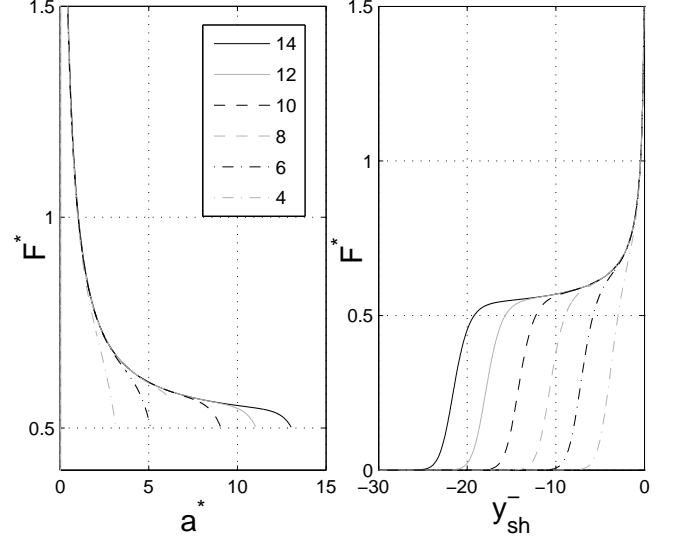


Figure 8. $F^* = (F^{\text{ATV}}/\bar{N})$ is plotted against the horizon area $\mathbf{a}^* := (\mathbf{a}_{\text{GDH}}/\bar{N})$ (left) and y_{sh}^- (right) for values of M^* from 4 to 14. For all M^* values, F^* starts at the value of 0 at the distant past ($\kappa y_{\text{sh}}^- \ll -1$), and then joins a universal curve of F^* . Note that once the GDH is formed, (the rightmost beginning of each curve on the left plot) F^* is already slightly larger in magnitude than the Hawking/thermal value 0.5 and it increases steadily as one approaches the last ray (i.e. as \mathbf{a}_{GDH} and y_{sh}^- approach 0).

the time dependence of y^- for various values of M^* is very similar but not identical. Recall, however, that there is some freedom in the definition of the affine parameter. In particular, in each space-time we can shift it by a constant, and the particular value of the constant can vary from one space-time to the next (e.g. depend on the ADM mass). This shift does not affect any of our considerations, including the balance law (2.14).

Let us define y_{sh}^- by shifting each y^- so that each solution reaches the same small non-zero value of the horizon area, $\mathbf{a}^* = \epsilon$, at the same y_{sh}^- . It turns out that this shift has the remarkable feature that, for initially macroscopic black holes, all shifted curves now coincide for *all* values of \mathbf{a}^* . Thus, we have a universal, monotonic function of \mathbf{a}^* plotted in Fig. 7, right. Hence y_{sh}^- also serves as an invariant time coordinate. In fact it has an advantage over \mathbf{a}_{GDH} : whereas \mathbf{a}^* is defined only after the first marginally trapped surface is formed (see Fig 2), y_{sh}^- is well defined throughout the mean-field space-time (M, g) .

Dynamical Universality of F^{ATV} and $M_{\text{Bondi}}^{\text{ATV}}$: We can repeat the procedure used above for y^- to investigate if dynamics of other physical quantities such as the Bondi flux $F^* := (F^{\text{ATV}}/\bar{N})$ and the Bondi mass $M_{\text{Bondi}}^* := (M_{\text{Bondi}}^{\text{ATV}}/\bar{N})$ are also universal. Note, however, that unlike y^- , there is no ‘shift’ (or indeed any other) freedom in the definitions of F^{ATV} and $M_{\text{Bondi}}^{\text{ATV}}$. So, if there is universality, it should emerge directly, *without any adjustments*, in the plots of F^* and M_{Bondi}^* against $\mathbf{a}^* = (\mathbf{a}_{\text{GDH}}/\bar{N})$ or y_{sh}^- .

Let us begin with the Bondi flux. Recall, first, that in the ex-

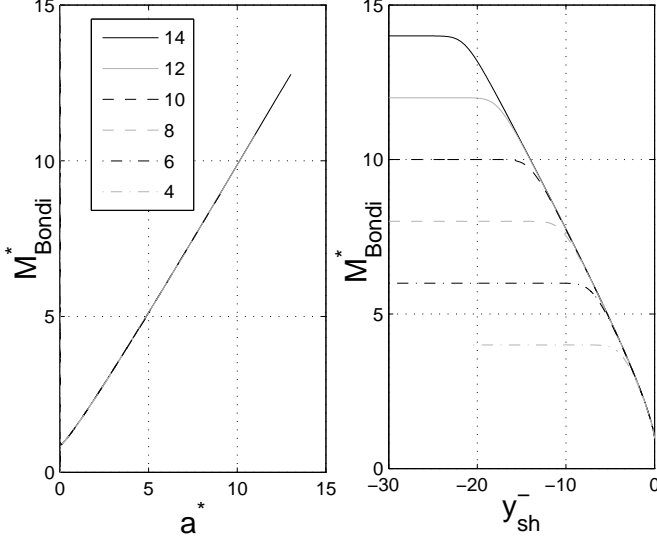


Figure 9. $M_{\text{Bondi}}^* = (M_{\text{Bondi}}^{\text{ATV}}/\bar{N})$ is plotted against the horizon area $a^* := (a_{\text{GDH}}/\bar{N})$ (left) and y_{sh}^- (right) for values of M^* from 4 to 14. For all these macroscopic M^* , M_{Bondi}^* starts at the value of M_{ADM} in the distant past ($\kappa y_{\text{sh}}^- \ll -1$), and then joins a universal curve of M_{Bondi}^* . When the dynamical horizon first forms M_{Bondi}^* is quite close to its initial value of M^* . (This is difficult to see in the left plot where all the curves crowd.) This means that almost all of the evaporation occurs after the formation of the dynamical horizon.

ternal field approximation [2, 26], the energy flux is very small in the distant past, rises steeply at $\kappa y^- \approx -\ln(GM_{\text{ADM}}/\kappa)$ and then quickly asymptotes to the Hawking value $F^{\text{Haw}} = (\bar{N}\hbar\kappa^2/2)$. This constant flux is characteristic of thermal radiation at temperature $\kappa\hbar$ in two space-time dimensions. In our simulations (with $N = 24$, or) $\bar{N} = 1$ and $\hbar = \kappa = 1$, it corresponds to $F^{\text{Haw}} = 0.5$.

In the mean-field theory, numerical simulations show that, for all initially macroscopic black holes, the energy flux $F^* := (F^{\text{ATV}}/\bar{N})$ is also negligibly small in the distant past and then rises steeply. But this rise is now associated with a clearly identifiable dynamical process: formation of the first marginally trapped surface. As we noted in section II B, for a shell collapse, analytical calculations show that the area of this first surface is given by (2.10). Assuming that we have a macroscopic initial mass, $M^* \gg \sqrt{G\hbar} M_{\text{Pl}} =: \tilde{M}_{\text{Pl}}$, Eq (2.10) simplifies:

$$a_{\text{initial}}^* \approx G\hbar \left[\frac{M^*}{\tilde{M}_{\text{Pl}}} - 1 + \frac{\tilde{M}_{\text{Pl}}}{2M^*} + \dots \right] \quad (3.6)$$

This relation is borne out in simulations. Assuming that the black hole is very large at this stage, heuristically, one can equate the area of this new born GDH with the Bondi mass at the retarded instant of time, say $y^- = y_o^-$, at which it is born. This implies that, per scalar field, only ~ 1 Planck unit of M_{Bondi}^* has been radiated over the long period of time from $y^- = -\infty$ till $y^- = y_o^-$. But once the GDH appears, the flux rises steeply to a value close to but higher than 0.5. Then, it joins a universal curve all the way to the last ray where the area

a^* shrinks to zero. Thus, after a brief transient phase around the time the GDH is first formed, the time-dependence of the Bondi flux is universal. Fig. 8, left shows this universal time dependence with a^* as time and Fig. 8, right shows it with y_{sh}^- as time.

In virtue of the balance law (2.14) one would expect this universality to imply a universal time dependence also for the Bondi mass M_{Bondi}^* . This is indeed the case. At spatial infinity i_{R}^o , we have $M_{\text{Bondi}}^* = M^*$. There is a transient phase around the birth of the GDH in which the Bondi mass decreases steeply. Quickly after that, the time dependence of M_{Bondi}^* follows a universal trajectory until the last ray. Fig. 9, left shows this universality with a^* as time while Fig. 9, right shows it with y_{sh}^- as time.

To summarize, using either a^* or y_{sh}^- as an invariant time coordinate, we can track the dynamics of F^* and M_{Bondi}^* . In each of the four cases, there is a universal curve describing these dynamics. For definiteness let us use a^* as time and focus on M_{Bondi}^* (the situation is the same in the other three cases). Since both quantities are positive, let us consider the time-mass quadrant they span. Fix a very large initial black hole with $M^* = M_o^*$ and denote by c_o the curve in the quadrant that describes its time evolution. Then, given any other black hole with $M^* < M_o^*$, the curve c describing the dynamical evolution of its M_{Bondi}^* starts out at a smaller value of time (i.e. a^*) marking the birth of the GDH of that space-time and, after a brief transient phase, joins the curve c_o all the way until its horizon shrinks to zero. Here we have focused on the ATV flux and mass because their properties make them physically more relevant. But this universality holds also for the flux and mass expressions, F^{Trad} , $M_{\text{Bondi}}^{\text{Trad}}$ that have been traditionally used in the literature.

Curvature at the last ray: There has been considerable discussion on the nature of geometry at the last ray. Since this ray starts out at the singularity, a natural question is whether a curvature singularity propagates out all along the last ray to \mathcal{I}_{R}^+ . This would be a ‘thunderbolt’ representing a singular Cauchy horizon [20]. If it were to occur, the evolution across the last ray would not just be ambiguous; it would be impossible. However, *a priori* it is not clear that a thunderbolt would in fact occur. For, the ‘strength’ of the singularity goes to zero at its right end point where the last ray originates.

Using numerical simulations, Hawking and Stewart [20] argued that a thunderbolt does occur in the semi-classical theory. But they went on to suggest that it could be softened by full quantum gravity, i.e., that full quantum gravity effects would tame it to produce possibly a very intense but finite burst of high energy particles in the full theory.

Our calculation of the Ricci scalar very close to the last ray shows that, except for a small region near the singularity, the scalar curvature at the last ray is *not* large (Fig. 3). Thus, our more exhaustive and high precision calculations rule out a thunderbolt singularity in the original sense of the term. This overall conclusion agrees with the later results in [18]. (Both these calculations were done only for initially microscopic black holes while results hold also for macroscopic ones.) However, our calculations show that the flux F^{ATV} does increase very steeply near the last ray (see Fig. 8). Nu-

merically, we could not conclude whether the flux remains finite at the last ray or diverges. However, the integrated flux which determines the change in $M_{\text{Bondi}}^{\text{ATV}}$ is indeed finite and in fact *not very significant* in the region very near the last ray. For macroscopic M^* values, the total radiated energy after the point when F^* reaches the value 1 is ~ 1 Planck mass. (see Figs. 8, 9). Thus, if we were to associate the thunderbolt idea to the steep increase of flux at the last ray, this would have to be in quite a weak sense; in particular, there is no singular Cauchy horizon.

Nature of the Bondi flux: Recall that in the external field approximation, the energy flux starts out very low, rapidly increases and approaches the constant thermal value $(F^{\text{Haw}}/\bar{N}) = \hbar\kappa^2/2$ ($= 0.5$ in our simulations) from below [2, 26]. In the mean-field theory, the flux F^{ATV} also starts out very small and suddenly increases when the GDH is first formed. However, it overshoots the thermal value and ceases to be constant much before the black hole shrinks to Planck size (Fig. 8). During subsequent evolution, F^{ATV} monotonically increases in magnitude and is about 70% greater than the constant thermal value F^{Haw} when $M_{\text{Bondi}}^{\text{ATV}} \sim 2\bar{N}M_{\text{Pl}}$: the standard assumption that the flux is thermal till the black hole shrinks to Planck size is not borne out in the mean field theory. (One's 4-dimensional intuition may lead one to think that the increase in the flux merely reflects that the black hole gets hotter as it evaporates; but this is not so because the temperature of a CGHS black hole is an *absolute constant*, $T_{\text{Haw}} = \kappa\hbar$). In the interval between the formation of the GDH and the time when $M_{\text{Bondi}}^{\text{ATV}}$ approaches $\bar{N}M_{\text{Pl}}$, the numerical flux is well approximated by

$$F^{\text{ATV}} = F^{\text{Haw}} \left[1 - \ln \left(1 - \frac{\bar{N}M_{\text{Pl}}}{M_{\text{Bondi}}^{\text{ATV}}} \right) \right]. \quad (3.7)$$

Thus, in this interval the flux is close to the constant thermal value only while the area a of the GDH is much greater than \bar{N} Planck units.¹⁰

C. Universality beyond the shell collapse.

So far, we have focused our attention on a delta distribution shell collapse (2.8). As we will discuss more in the following section IV, we expect the results to be robust for a large class of infalling profiles, so long as the GDH forms promptly. To

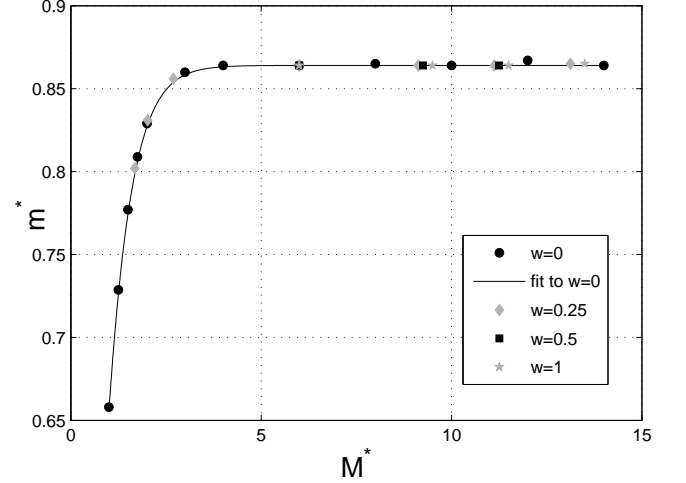


Figure 10. The value of m^* (i.e. $M_{\text{Bondi}}^{\text{ATV}}/\bar{N}$ at the last ray) plotted against M^* (which equals M_{ADM}/\bar{N}) for $M^* \geq 1$. In addition to points corresponding to shell collapse ($w = 0$) the plot now includes points with more general profiles with $w = 0.25, 0.5, 1$. The universal value $m^* \approx 0.864$ persists for $M^* \geq 4$.

test this conjecture, we evolved a 2-parameter family of initial data, parameterized by a characteristic initial mass M and width w . Now, it is clear from the form (2.6), (2.7) of initial data that what matters is not the profile $f_+^{(o)}$ itself but rather the integral of $(\partial_+ f_+^{(o)})^2$. We will specify it using two parameters, M and w :

$$\int_0^{\bar{x}^+} d\bar{x}^+ (\frac{\partial f_+^{(o)}}{\partial \bar{x}^+})^2 = \begin{cases} \frac{M}{12N} \left(1 - e^{-\frac{(\kappa \bar{x}^+ - 1)^2}{w^2}} \right)^4 & \bar{x}^+ > 1 \\ 0 & \bar{x}^+ < 1 \end{cases} \quad (3.8)$$

This choice is motivated by the following considerations. First, as in the shell collapse, there is a neighborhood of \mathcal{I}_L^- in which the solution represents the vacuum of the theory. Second, the power 4 on the right side is chosen to ensure high differentiability at $x^+ = 1$ (i.e. $z^+ = 0$). Thus, $f_+^{(o)}$ is \mathcal{C}^4 and furthermore decays faster than $e^{-C\kappa z^+}$ for any C as $z^+ \rightarrow \infty$. Third, the parameter w provides a measure of the width of the matter profile in x^+ coordinates, which is roughly the width in z^+ for $w \lesssim 1$. Finally, note that we recover the shell profile in the limit $w \rightarrow 0$ and expect that the physical requirement of a ‘prompt collapse’ will be met for sufficiently small w . In the case of a shell profile (2.8), the parameter M represents the ADM mass. A simple calculation shows that for a general profile in family (3.8), M_{ADM} is given by a function of the two parameters: $M_{\text{ADM}} = M(1 + 1.39w)$. Thus, within this family, the issue of universality of a physical quantity boils down to the question of whether it depends only on the specific combination $M(1 + 1.39w)$ of the two parameters.

Numerical evolutions were carried out for $M^* \approx 6, 9, 11, 13$ and $w = 0.25, 0.5, 1$. We find that universality is indeed retained for all these cases. Specifically, we repeated the following analysis of section IIIB for various values of

¹⁰ The leading order correction $+(\bar{N}M_{\text{Pl}}/M_{\text{Bondi}})$ to the Hawking flux was obtained by Ori by analytical approximation methods and served as the point of departure for obtaining the fit (3.7). Note also that if the fluxes differ over a significant time interval, it follows that the quantum radiation is not thermal. But the converse is not true as there are *pure* states in the outgoing Hilbert space for which the energy flux at \mathcal{I}_R^+ is extremely well approximated by the constant thermal value. For quantum states, what matters is the comparison between the function $y_{\text{sh}}^-(z^-)$ and its classical counterpart $\underline{y}^-(z^-)$ given by (3.1) [7, 8]. And these two functions are very different. Finally, nonthermal fluxes were also observed in a quantum model of four-dimensional spherical shell collapse [27]

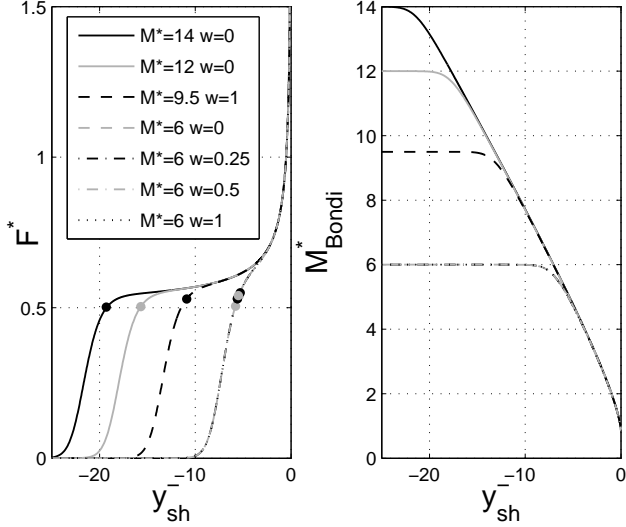


Figure 11. F^* (left) and M_{Bondi}^* (right) plotted against y_{sh}^- , for various incoming matter profiles (w and M_{ADM} values), including several shell ($w = 0$) cases. The time when the dynamical horizon first forms is marked on each flux curve (which is later for larger w). All the curves with the same M_{ADM} (6 in this example) are on top of each other and cannot be distinguished by the eye, showing that they have the same universal behavior throughout the evolution, including the early times. More generally all the asymptotic physical quantities depend only on the combination M_{ADM} of the profile parameters M and w as long as κw is small compared to the initial area of the GDH.

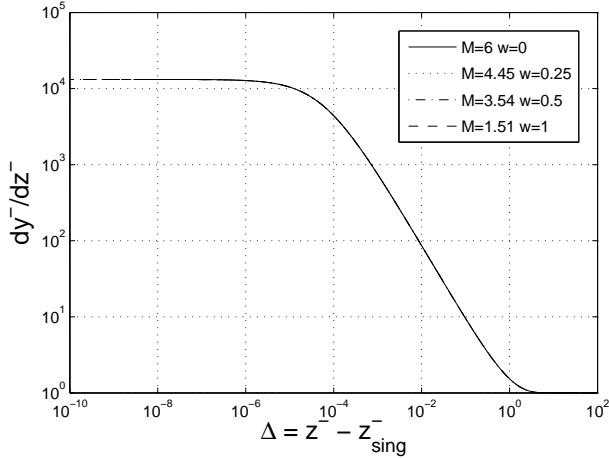


Figure 12. Plot of dy^-/dz^- against the separation in z^- from the singularity for various values of M and w with a fixed ADM mass $M^* = 6$. The functional dependence $y^-(z^-)$ determines the physics of the outgoing quantum state completely [7, 8]. Coincidence of these curves in the mean-field theory suggests that the outgoing quantum state is likely to be universal within the class of initial data with the same ADM mass, so long as the collapse is prompt.

M and w :

- i) The relationship between the end-point values m^* of M_{Bondi}^* against M^* ; see Fig. 10. For $M^* \geq 4$, we again find m^* has the same universal value, $\sim .864 M_{\text{Pl}}$.
- ii) The relationship of y^- vs a^* (once GDH becomes time-like). As before, by an appropriate shift, we find a y_{sh}^- that can be used as a universal time coordinate for all cases.
- iii) The dependence of F^* and M_{Bondi}^* on a^* and y_{sh}^- ; see Fig. 11. For a fixed value of M_{ADM} the plots are indistinguishable, so that even for this broader class of matter profiles, there are two universal curves, one for the dynamics of F^* and the other for M_{Bondi}^* . In particular, for a given $w > 0$, the time evolution F^* and M_{Bondi}^* is identical to that obtained with the shell collapse ($w = 0$).

In the classical theory, if the collapsing matter $f_+^{(o)}$ is compactly supported on \mathcal{I}_R^- , to the future of this support the geometry is universal, determined by the ADM mass M_{ADM} . This is because stationary, classical, CGHS black holes are characterized completely by M_{ADM} . Whether the situation would have a direct counterpart in the semi-classical theory is not *a priori* clear because the semi-classical solutions are not stationary and there is no reason to expect the solution to be characterized just by one or two parameters to the future of the support of $f^{(o)}$. Our results provide a precise sense in which universality does persist. As long as the black hole is initially macroscopic and the collapse is prompt, we have : i) a universal asymptotic time translation $\partial/\partial y_{\text{sh}}^-$ (Fig 12); and, soon after the formation of the GDH, ii) universal dynamics of physical observables with respect to the physical asymptotic time y_{sh}^- .

IV. DISCUSSION

The CGHS model provides a useful arena to explore the formation and quantum evaporation of black holes. For, the classical action is closely related to that governing the spherically symmetric gravitational collapse in 4 dimensions and, at the same time, the decoupling of matter and dilaton fields in the model introduces significant technical simplification. However, in this paper, we were not concerned with the *full* quantum theory of the CGHS model. Rather, we restricted ourselves to the mean-field equations of [7, 8] and explored their implications using high precision numerics.

A. Viewpoint

Our analysis was carried out in the same spirit that drove the investigation of critical phenomena in classical general relativity [5, 6]. There, one takes equations of general relativity seriously and shows, for example, that black holes can form with arbitrarily small mass. From a more complete physical perspective, these black holes would have enormous Hawking temperature, whence quantum effects would be crucial. To know whether black holes with arbitrarily small masses can form in Nature, one cannot really rely on the classical

Einstein equations. The viewpoint in those investigations was rather that, since general relativity is a self-contained, well defined theory, it is interesting to explore what it has to say about such conceptual issues. The results of those explorations led to the discovery of critical behavior in gravitational collapse, which is of great interest from a theoretical and mathematical physics perspective. In the same vein, in the CGHS model, it is conceivable [8] that the relative quantum fluctuations of operators $\hat{\Theta}$, $\hat{\Phi}$, may become of order 1 once the horizon mass is of the order of, say, $\sqrt{M^* M_{\text{Pl}}}$.¹¹ Suppose this were to happen at a point p on the GDH. Then, to the future of the null ray from p to \mathcal{I}_R^+ , solutions Θ , Φ to the mean-field equations discussed in this paper would be poor approximations of the expectation values of $\hat{\Theta}$, $\hat{\Phi}$ that result from full quantum equations. That is, our solutions to the mean-field equations would not be *physically* reliable in this future region. The scope of this paper did not include this issue of the physical domain of validity of the mean-field approximation. As in much of the literature on semi-classical gravity, we considered the entire space-time domain where the mean-field equations have unambiguous solutions. And as in investigations of critical phenomena, our focus was on exploring non-trivial consequences of these equations. Specifically, we wished to explore two questions: *Are standard expectations about predictions of semi-classical gravity borne out? Do the mean-field dynamics exhibit any universal features?*

B. Summary and conjectures in geometric analysis

We found that some of the standard expectations of semi-classical gravity are indeed borne out: The semi-classical space-time is asymptotically flat at \mathcal{I}_R^+ as in the classical theory, but in contrast to the classical case \mathcal{I}_R^+ is now *incomplete*. Thus, the expectation [25] that the full quantum space-time would be an extension of the semi-classical one is viable.

However, a number of other expectations underlying the standard evaporation paradigm turned out to be incorrect. Specifically:

- a) The traditional Bondi mass $M_{\text{Bondi}}^{\text{Trad}}$ is large and negative at the end of the semi-classical evaporation rather than of Planck size and positive;
- b) The recently introduced Bondi mass $M_{\text{Bondi}}^{\text{ATV}}$ remains positive but is large, rather than of Planck size at the end of evaporation;
- c) The energy flux F^{ATV} of quantum radiation deviates from the Hawking flux corresponding to thermal radiation even when the black hole is macroscopic, the deviation becoming larger as the evaporation progresses; and,
- d) Along the ‘last ray’ from the end of the singularity to \mathcal{I}_R^+ , curvature remains finite; there is no ‘thunderbolt singularity’ in the metric extending to \mathcal{I}_R^+ .

¹¹ Note incidentally that in 4-dimensions, when a black hole with $M_{\text{ADM}} = M_\odot$ has shrunk down through quantum radiation to mass $\sqrt{M_{\text{ADM}} M_{\text{Pl}}}$, its horizon radius is less than a fermi, and for a super-massive black hole with $M_{\text{ADM}} = 10^9 M_\odot$, this radius is a tenth of an angstrom.

The analysis also brought out some unforeseen universalities. The most striking among them are:

- i) If $M^* = M_{\text{ADM}}/\tilde{N}$ is macroscopic, at the end of semi-classical evaporation $m^* := M_{\text{Bondi}}^{\text{ATV}}/\tilde{N}$ assumes a universal value, $m^* \approx .864 M_{\text{Pl}}$;
- ii) As long as M^* is greater than M_{Pl} , there is a universal relation: $m^* = \alpha(1 - e^{-\beta(M^*)^\gamma}) M_{\text{Pl}}$, with $\alpha \approx 0.864$, $\beta \approx 1.42$, $\gamma \approx 1.15$;
- iii) An appropriately defined affine parameter y_{sh}^- along \mathcal{I}_R^+ is a universal function of the area a_{GDH} of the generalized dynamical horizon;
- iv) The evolution of the Bondi mass $M_{\text{Bondi}}^{\text{ATV}}$ with respect to an invariantly defined time parameter a_{GDH} (or y_{sh}^-) follows a universal curve (and same is true for the energy flux F^{ATV}).

These results bring out a point that has not drawn the attention it deserves: the number N of fields plays an important role in distinguishing between macroscopic and Planck size quantities. If semi-classical gravity is to be valid in an interesting regime, we must have $N \gg 1$ and the ADM mass and horizon area are macroscopic if $M_{\text{ADM}}/\tilde{N} \geq 4G\hbar M_{\text{Pl}}$ and $a/\tilde{N} \geq G\hbar$. (By contrast, it has generally been assumed that the external field approximation should hold so long as $M_{\text{ADM}} > M_{\text{Pl}}$ or $a > G\hbar$.) Of course the ADM masses can be much larger and for analogs of astrophysical black holes we would have $M_{\text{ADM}}/(\tilde{N} M_{\text{Pl}}) \gg G\hbar$. After a brief transient period around the time the GDH is born, dynamics of various physical quantities exhibit universal behavior till the horizon area a goes to zero. If $M_{\text{ADM}}/(\tilde{N} M_{\text{Pl}}) \gg 1$, the universal behavior spans a huge interval of time, as measured by the physical affine parameter y_{sh}^- on \mathcal{I}_R^+ or the horizon area a .

All these features are direct consequences of the dynamical equations (2.1) and (2.2) for infalling profiles (3.8) characterized by two parameters M, w . Of course, with numerical analysis one cannot exhaustively cover the full range of solutions, and given the complete freedom to specify incoming flux from \mathcal{I}_R^- one can always construct initial data that will not exhibit our universal dynamics—for example, after the GDH is formed, send in a steady stream of energy with magnitude comparable to F^{ATV} . Here we have restricted attention to initial data for which the GDH forms *promptly*, and is then left to decay quantum mechanically without further intervention. Our intuition is that universality is associated with a *pure quantum decay* of a GDH, pure in the sense that the decay is uncontaminated by continued infall of classical matter carrying positive energy. Therefore, we conjecture that for macroscopic black holes formed by smooth infalling matter profiles of compact support, these universalities will continue to hold soon after the GDH turns time-like. More generally, for profiles in which the positive energy flux carried across the GDH by the classical fields $f_+^{(i)}$ is negligible compared to the negative quantum flux to the future of some ray $z^+ = z_o^+$, the universality should also hold in the future region $z^+ > z_o^+$.

This scenario provides a number of concrete and interesting problems for the geometric analysis community. Start with initial data (2.6), (2.7) at \mathcal{I}^- with $f_-^{(i)} = 0$ and a smooth profile f_+^o with compact support for each of the N fields $f_+^{(i)}$. Evolve them using (2.1) and (2.2). Then, we are led to con-

jecture that the resulting solution has the following properties:

- 1) The maximal solution is asymptotically flat at right future null infinity \mathcal{I}_R^+ ;
- 2) \mathcal{I}_R^+ is future incomplete;
- 3) A positive mass theorem holds: The Bondi mass $M_{\text{Bondi}}^{\text{ATV}}$ is non-negative everywhere on \mathcal{I}_R^+ ;
- 4) So long as $M_{\text{ADM}} \gg \bar{N} \sqrt{\hbar/G} \kappa$, the final Bondi mass (evaluated at the last ray) is given by $M_{\text{Bondi}}^{\text{final}} \approx 0.864 \bar{N} \sqrt{\hbar/G} \kappa$;
- 5) Fix a solution s_o with $M_{\text{ADM}} = M_o \gg N_o \sqrt{\hbar/G} \kappa$ and consider the curve c_o describing the time evolution of the Bondi mass in the $a_{\text{GDH}}/N_o - M_{\text{Bondi}}/N_o$ plane it defines. Then the corresponding curve c for a solution with $M/N < M_o/N_o$ coincides with c_o soon after its GDH becomes time-like.

C. Quantum Theory

Although the mean-field approximation ignores quantum fluctuations of geometry, nonetheless our results provide some intuition on what is likely to happen near \mathcal{I}_R^+ in the full quantum theory. First, because there is no thunderbolt singularity along the last ray, the semi-classical solution admits extensions in a large neighborhood of \mathcal{I}_R^+ to the future of the last ray. In the mean-field approximation the extension is ambiguous because of the presence of a singularity along which the metric is C^0 but not C^1 . But it is plausible that these ambiguities will be resolved in the full quantum theory and there is some evidence supporting this expectation [8, 28]. What features would this quantum extension have? Recall that the model has N scalar fields and the black hole emits quantum radiation in each of these channels. The Bondi mass that is left over at the last ray is $M_{\text{Bondi}} \approx 0.864 \bar{N} M_{\text{Pl}}$. So we have $(0.864/24) M_{\text{Pl}}$ units of mass left over *per channel*. It is generally assumed that this tiny remainder will be quickly radiated away across $\bar{\mathcal{I}}_R^+$, the right future null infinity of the quantum space-time that extends beyond the last ray. Suppose it is radiated in a finite affine time. Then, there is a point p on $\bar{\mathcal{I}}_R^+$ beyond which $M_{\text{Bondi}}^{\text{ATV}}$ and F^{ATV} both vanish. The expression (2.16) of F^{ATV} now implies that $\bar{\mathcal{I}}_R^+$ is ‘as long as’ \mathcal{I}_L^- . This is sufficient to conclude that the vacuum state (of right moving fields $\hat{f}_{-}^{(i)}$) on \mathcal{I}_L^- evolves to a pure state on $\bar{\mathcal{I}}_R^+$ (because there are no modes to trace over). This is precisely the paradigm proposed in [7]. Thus, the semi-classical results obtained in this paper provide concrete support for that paradigm and re-enforces the analogous 4-dimensional paradigm of [29] (which was later shown to be borne out also in the asymptotically AdS context in string theory [30]).

All our analysis was restricted to the 2-dimensional, CGHS black holes. As we mentioned in section I, while they mimic several features of 4-dimensional black holes formed by a spherical symmetric collapse of scalar fields, there are also some key differences. We will conclude with a list of the most important of these differences and briefly discuss their consequences. (For a more detailed discussion, see [8].)

First, in 2-dimensions, surface gravity κ and hence, in the

external field approximation, the Hawking temperature T_{Haw} , is a constant of the theory; it does not depend on the specific black hole under consideration. In 4-dimensions, by contrast, κ and T_{Haw} depend on the black hole. In the spherical case, they go inversely as the mass so one is led to conclude that the black hole gets hotter as it evaporates. A second important difference is that, in the CGHS black hole, matter fields $f^{(i)}$ are decoupled from the dilaton and their propagation is therefore decoupled from the dynamics of the geometric sector. This then implies that the right and left moving modes do not talk to one another. In 4 dimensions, the $f^{(i)}$ are directly coupled to the dilaton and their dynamics cannot be neatly separated from those of geometric fields Φ, Θ . Hence technically the problem is much more difficult. Finally, in 4 dimensions there is only one \mathcal{I}^+ and only one \mathcal{I}^- while in 2 dimensions each of them has two distinct components, right and left. Conceptually, this difference is extremely important. In 2 dimensions the infalling matter is only in the plus modes, $f_{+}^{(i)}$, and its initial state is specified just on \mathcal{I}_R^- while the outgoing quantum radiation refers to the minus modes, $f_{-}^{(i)}$, and its final state has support only on \mathcal{I}_R^+ . In 4-dimension, there is no such clean separation.

What are the implications of these differences?

Because of the first two differences, analysis of CGHS black holes is technically simpler and this simplicity brings out some features of the evaporation process that can be masked by technical complications in 4 dimensions. For instance, since the Hawking temperature T_{Haw} is an absolute constant ($\hbar\kappa$) for CGHS black holes, the standard paradigm that the quantum radiation is thermal till the black hole has shrunk to Planck size leads to a clean prediction that the energy flux should be constant, $F^{\text{Haw}} = \hbar\kappa^2/48$. We tested this simple prediction in the mean field approximation and found that it does not hold even when the horizon area is macroscopic. In 4 dimensions, since the temperature varies as the black hole evaporates, testing the standard paradigm is much more delicate. Similarly, thanks to the underlying technical simplicity in the CGHS case, we were able to discover scaling properties and universalities. We believe that some of them, such as the ‘end point universality’, will have counterparts in 4 dimensions but they will be harder to unravel. The CGHS results provide hints to uncover them.

The third difference has deeper conceptual implications which we will now discuss in some detail. In 4-dimensions, since there is a single \mathcal{I}^- and a single \mathcal{I}^+ , unitarity of the quantum S-matrix immediately implies that all the information in the incoming state can be recovered in the outgoing state. In 2 dimensions, on the other hand, there are two distinct questions: i) is the S-matrix from \mathcal{I}_L^- to \mathcal{I}_R^+ unitary? and ii) is the information about the infalling matter on \mathcal{I}_R^- recovered in the outgoing state at \mathcal{I}_R^+ ? As discussed above, results of this paper strongly support the paradigm of [7, 8] in which the answer to the first question is in the affirmative; information on \mathcal{I}_L^- is faithfully recovered on \mathcal{I}_R^+ . However, this does *not* imply that all the infalling information at \mathcal{I}_R^- is imprinted on the outgoing state at \mathcal{I}_R^+ .

In the early CGHS literature, this second issue was often

mixed with the first one. Because it was assumed that all (or at least most) of the ADM mass is evaporated away through quantum radiation, it seemed natural to consider seriously the possibility that all the information in the infalling matter at \mathcal{I}_R^- can be recovered from the outgoing quantum state at \mathcal{I}_R^+ . The key question was then to find mechanisms that make it possible to transfer the information in the *right-moving* infalling modes $f_+^{(i)}$ to the *left-moving* modes $f_-^{(i)}$ going out to \mathcal{I}_R^+ . In [14], for example, the 2 dimensional Schwinger model with a position dependent coupling constant was discussed in some detail to suggest a possible mechanism.

However, our universality results strongly suggest that these attempts were misdirected. The physical content of the outgoing *quantum* state is encoded entirely in the function $y_{\text{sh}}^-(z^-)$ [7, 8] on \mathcal{I}_R^+ , the right future null infinity of the quantum extension of the semi-classical space-time. In the family of profile functions $f_+^{(o)}$ we analyzed in detail, the function $y_{\text{sh}}^-(z^-)$ on \mathcal{I}_R^+ has universal behavior, determined just by the total ADM mass. Since only a tiny fraction of Planck mass is radiated per channel in the portion of \mathcal{I}_R^+ that is not already in \mathcal{I}_R^+ , it seems highly unlikely that the remaining information can be encoded in the functional form of $y_{\text{sh}}^-(z^-)$ in that portion. Thus, at least for large M^* we expect the answer to question ii) to be in the negative: information contained in the general infalling matter profile on \mathcal{I}_R^- will *not* be fully recovered at \mathcal{I}_R^+ . From our perspective, this is not surprising be-

cause the structure of null infinity in the CGHS model is rather peculiar from the standpoint of 4 dimensions where much of our intuition is rooted. In 2 dimensional models, \mathcal{I}_R^+ is not the *full* future boundary of space-time. Yet discussions of CGHS black holes generally ignore \mathcal{I}_L^{o+} because, as we saw in section I, even in the classical theory the black hole interpretation holds only with reference to \mathcal{I}_R^+ . Indeed, for this reason, investigations of quantum CGHS black holes have generally focused on the Hawking effect and question i) of unitarity, both of which involve dynamics only of $\hat{f}_-^{(i)}$ for which \mathcal{I}_R^+ does effectively serve as the complete future boundary.

In 4 dimensions, the situation is qualitatively different in this regard: in particular, the outgoing state is specified on all of future null infinity \mathcal{I}^+ , not just on half of it. Therefore, if the singularity is resolved in the full quantum theory, \mathcal{I}_R^+ *would* be the complete future boundary of the quantum space-time and there would be no obstruction for the S matrix to be unitary and hence for the full information on \mathcal{I}^- to be imprinted in the outgoing state on \mathcal{I}^+ .

Acknowledgements: We would like to thank Amos Ori, Madhavan Varadarajan for discussions and for their comments on our manuscript. This work was supported by the NSF grants PHY-0745779, PHY-0854743, the Eberly research funds of Penn State, and the Alfred P. Sloan Foundation.

-
- [1] C. G. Callan, S. B. Giddings, J. A. Harvey and A. Strominger, Evanescent black holes, Phys. Rev. D **45**, R1005-R1009 (1992).
 - [2] Quantum mechanics of black holes, S. B. Giddings, arXiv:hep-th/9412138; A. Strominger, les Houches lectures on black holes, arXiv:hep-th/9501071
 - [3] G. Mandal, A. M. Sengupta and S. R. Wadia, Classical solutions of 2-dimensional string theory, Modern Physics Letters **A6**, 1685-1696 (1991)
E. Witten, String theory and black holes, Phys. Rev. D **44**, 314-324 (1991)
 - [4] A. Ashtekar, F. Pretorius and F. M. Ramazanoğlu, Surprises in the Evaporation of 2-Dimensional Black Holes, arXiv:1011.6442v1
 - [5] M. Choptuik, Universality and scaling In Gravitational collapse of a massless scalar field, Phys. Rev. Lett. **70**, 9 (1993).
 - [6] C. Gundlach and J. M. Martin-Garcia, Critical phenomena in gravitational collapse, LivingRev. Rel. **10**:5 (2007)
 - [7] A. Ashtekar, V. Taveras and M. Varadarajan, Information is not lost in the evaporation of 2-dimensional black holes, Phys. Rev. Lett. **100**, 211302 (2008)
 - [8] M. Varadarajan, A. Ashtekar and V. Taveras (pre-print, 2010)
 - [9] F. M. Ramazanoğlu and F. Pretorius, Two-dimensional quantum black holes: Numerical methods, Class. Quantum Grav. **27**, 245027 (2010)
 - [10] R. P. Geroch and G. T. Horowitz, asymptotically simple does not imply asymptotically Minkowskian, Phys. Rev. Lett. **40**, 203-206 (1978)
 - [11] A. Ori, Approximate solution to the CGHS field equations for two-dimensional evaporating black holes, Phys. Rev. D **82**, 104009 (2010)
 - [12] T. Piran and A. Strominger, Numerical analysis of black hole evaporation, Phys. Rev. D **48**, 4729-4734 (1993)
 - [13] H. Bondi, M. G. J. Van den Berger, and A. W. K. Metzner, Gravitational waves in general relativity VIII. Waves from axisymmetric isolated systems, Proc. Roy. Soc. (London) **A269** 21-52 (1962)
 - [14] L. Susskind and L. Thorlacius, Hawking radiation and back reaction, Nucl. Phys. B **382**, 123-147 (1992)
 - [15] S. Hayward, Cosmic censorship in 2-dimensional dilaton gravity, Class. Quant. Grav. **10**, 985-994 (1993).
 - [16] A. Ashtekar and B. Krishnan, Isolated and dynamical horizons and their applications, LivingRev. Rel. **7**:10 (2004)
 - [17] A. Ashtekar and B. Krishnan, Dynamical horizons: Energy, angular momentum and balance laws, Phys. Rev. Lett. **89**, 261101 (2002);
Dynamical horizons and their properties, Phys. Rev. D **68** 104030 (2003)
 - [18] D. A. Lowe, Semiclassical approach to black hole evaporation, Phys. Rev. D **47**, 2446-2453 (1993)
 - [19] T. Tada and S. Uehara, Consequences of Hawking radiation from 2-d dilaton black holes, Phys. Rev. D **51** 4259-4264 (1995)
 - [20] S. W. Hawking and J. M. Stewart, Naked and thunderbolt singularities in black hole evaporation, Nucl. Phys. **B 400**, 393-415 (1993)
 - [21] D. Yeom and H. Zoe, Semi-classical black holes with large N re-scaling and information loss problem arXiv:0907.0677v1.
 - [22] J. G. Russo, L. Susskind and L. Thorlacius, The Endpoint of

- Hawking radiation, Phys. Rev. D **46**, 3444 (1992)
- [23] A. Bilal and C. G. Callan, Liouville models of black hole evaporation, Nucl. Phys. B **394**, 73 (1993)
 - [24] A. Strominger, Unitary rules for black hole evaporation, arXiv:hep-th/9410187.
 - [25] S. W. Hawking, particle creation by black holes, commun. Math. Phys. **43**, 199-220 (1975)
 - [26] S. B. Giddings and W. M. Nelson, Quantum emission of 2-dimensional black holes, Phys. Rev. D **46**, 2486-2496
 - [27] T. Vachaspati and D. Stojkovic, Quantum Radiation from Quantum Gravitational Collapse, Phys. Lett. B **663**, 107 (2008)
 - [28] D. Levanony and A. Ori, Interior design of a two-dimensional semiclassical black hole: Quantum transition across the singularity, Phys. Rev. D **81**, 104036 (2010) (1992)
 - [29] A. Ashtekar and M. Bojowald, Black hole evaporation: A paradigm, Class. Quant. Grav. **22**, 3349-3362 (2005)
 - [30] G. Horowitz, A. Lawrence and E. Silverstein, Insightful D-branes, JHEP 0907:057 (2009)